Accepted Manuscript

Synthesis, Biological Evaluation and Modeling Studies of Terphenyl Topoisomerase IIα Inhibitors as Anticancer Agents

Jin Qiu, Baobing Zhao, Wanxia Zhong, Yuemao Shen, Houwen Lin

PII: S0223-5234(15)00169-5

DOI: 10.1016/j.ejmech.2015.03.010

Reference: EJMECH 7755

To appear in: *European Journal of Medicinal Chemistry*

Received Date: 2 December 2014

Revised Date: 4 March 2015

Accepted Date: 4 March 2015

Please cite this article as: J. Qiu, B. Zhao, W. Zhong, Y. Shen, H. Lin, Synthesis, Biological Evaluation and Modeling Studies of Terphenyl Topoisomerase IIα Inhibitors as Anticancer Agents, *European Journal of Medicinal Chemistry* (2015), doi: 10.1016/j.ejmech.2015.03.010.

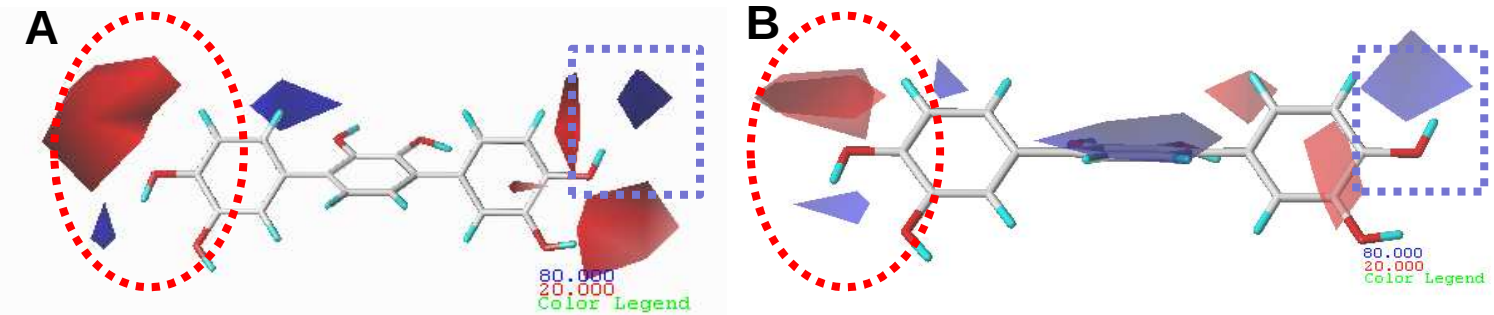

CoMFA contour map CoMSIA contour map

CoMFA and CoMSIA contour maps with compound **17** provide useful insight into designing novel TOP inhibitory.

Synthesis, Biological Evaluation and Modeling Studies of Terphenyl Topoisomerase IIα Inhibitors as Anticancer Agents

Jin Qiu,[a, §] Baobing Zhao,[b,§] Wanxia Zhong,[a,§] Yuemao Shen,[b,*] Houwen Lin[a,* *]

[a]Renji Hospital, School of Medicine, Shanghai Jiao Tong University, Pujian Road 160, Shanghai 200127, People's Republic of China

[b]Key Laboratory of Chemical Biology (Ministry of Education), School of Pharmaceutical Sciences, Shandong University, No. 44 West Wenhua Road, Jinan, Shandong 250012, People's Republic of China

[§]These authors contributed equally to this work.

* Corresponding author. Tel.: +86-531-88382108

** Corresponding author. Tel.: +86-021-68383346

E-mail addresses: yshen@sdu.edu.cn. (Yuemao Shen), franklin67@126.com (Houwen Lin)

ABSTRACT

We report the synthesis and evaluation of a series of novel terphenyls. Compound **17** had the most potent anticancer activity, indicating that the phenolic hydroxyl was a key group. A DNA relaxation test showed that compound **17** had a strong inhibitory effect on TOP2α, but not on TOP1, which was consistent with the docking analysis results. We performed a 3D-QSAR study using CoMFA and CoMSIA to determine, for the first time, the chemical-biological relationship in the inhibition of TOP by terphenyls. The CoMFA and CoMSIA model had good modeling statistics: leave-one-out q^2 of 0.605 and 0.622, r^2 of 0.998 and 0.994, and r^2_{pred} (test set) of 0.742 and 0.660. These results suggest that the ortho-phenolic hydroxyl on ring A is important for producing terphenyls with more efficacious activity.

Keywords: terphenyls; topoisomerase; 3D-QSAR

1. Introduction

Topoisomerases (TOP) are essential for managing the topological state of DNA [1, 2]. Several compounds may increase TOP-mediated DNA duplex breakage and kill cancer cells [3]. Different types of compounds inhibited TOP were reported recently, such as 2-substituted amidoanthraquinones and benzoxazole-containing derivatives inhibited TOP1 [4], fluorinated purine analogues [5] and dihydroxylated 2,4-diphenyl-6-thiophen-2-yl pyridine derivatives inhibited TOP2 [6], hydroxylated 2,4-diphenyl indenopyridine derivatives inhibited TOP2α [7]. Type II topoisomerases (TOP2s) are notable antitumor targets because they can transiently cleave both strands of a DNA duplex to enable the transport of another DNA segment [8]. TOP2α, one of the TOP2 isoforms, is highly expressed in rapidly growing cancer cells [9, 10]. Therefore, TOP2α is considered to be an important therapeutic target for developing TOP2α-targeting antitumor drugs [11, 12].

Recently, we discovered 8 *p*-terphenyl derivatives that have potent cytotoxicity against the human breast carcinoma MDA-MB-435 cell line, mediated through ROS generation, cell cycle arrest and apoptosis [13]. Compound [1,1':4',1"-Terphenyl]-2',3,3',4,4"-pentaol (**X1**, Figure 1) was found to only inhibit TOP2α activity, but not TOP1 [13]. Based on the structure of compound **X1**, we synthesized a series of novel terphenyls (Figure 1) and evaluated their cytotoxic activity against the MDA-MB-435 cell line (Table 1). Among these compounds, compound **17** was slightly more potent than **X1** (IC_{50} = 4.1 ± 0.39). As shown in Figure 2, the inhibitory activity of compound **17** against TOP2α was slightly stronger than that of VP-16 and its inhibitory activity against TOP2α and TOP1 was consistent with DOCK analysis results (Figure 3). To obtain a detailed and quantitative view of ligand binding, we used the comparative molecular field analysis (CoMFA) [14] and comparative molecular similarity indices analysis (CoMSIA) [15] methods. In this paper, for the first time, we report CoMFA and CoMSIA studies using a database of terphenyls that inhibit TOP. The QSAR models showed high quantitative correlations with good predictive abilities.

Figure 1.

Scheme 1-4..

2. Results

2.1. Chemistry

A series of terphenyls was synthesized as depicted in Schemes 1-4.

Scheme 1. The synthesis was started from commercially available 4-bromo-2-hydroxybenzoic acid and 5-bromosalicylic acid. These compounds were subjected to esterification and were coupled with 4,4,4',4',5,5,5',5'-octamethyl-2,2'-bi (1,3,2-dioxaborolane). This process resulted in compounds **21** and **22**. Then, these compounds were coupled with **23** [13] to obtain compounds **1** and **2** respectively. Using KOH to hydrolyze compounds **1** and **2** resulted in compounds **3** and **4**, respectively. Compounds **5** and **6** were obtained by the demethylation of **3** and **4** using boron tribromide.

Scheme 2. 1,4-dibromo-2,3-dimethoxybenzene (compound **24**) [13] was coupled with 3,4-dimethoxyphenylboronic acid to produce compound **25** and compound **16**, and the latter was demethylated to obtain compound **17**. Compound **25** was coupled with 4,4,4', 4', 5,5,5', 5'-octamethyl-2,2'-bi (1,3,2-dioxaborolane), without separation, and then was directly coupled with methyl 4-bromobenzoate (compound **26**) to obtain compounds **7**, **18** and **19**. Compound **7** was demethylated to produce compound **8**.

Scheme 3. 4-bromo-2-nitrophenol and 4,4,4',4',5,5,5',5'-octamethyl-2,2'-bi (1,3,2-dioxaborolane) were coupled through a Suzuki reaction; after the reaction was finished and without further treatment, a second reaction coupling the compound with 1,4-dibromo-2,3-dimethoxybenzene (compound **24**) was performed to obtain compounds **9** and **20**.

Scheme 4. Three equivalents of commercially available boric acid compounds (compounds **27**, **28** and **29**) were coupled with 1 equivalent of the corresponding brominated compounds (compound **24**, **30** and **31**) to obtain compounds **10**, **11**, **12**, **13** and **14**, respectively. Compound **15** was obtained by the demethylation of compound **12**.

2.2. Cytotoxicity evaluation of compounds 1-20 against MDA-MB-435 cells

Our previous studies had shown that the terphenyl compounds had more potent active on MDA-MB-435 cells line than on other cell lines, so we only use this cell line in this study. The

cytotoxicity of the compounds was expressed as IC_{50}, which is defined as the concentration of compound that results in 50% growth inhibition. Each value represents the mean ± SD of three independent experiments. The data are summarized in Table 1. These results demonstrate that the phenolic hydroxyl is a key group for activity and that the activities of compounds **3**, **4**, **5** and **8**, which had a substituted carboxyl group, were very low.

Table 1.

2.3. Inhibition of TOP2α

Compounds **2**, **12** and **17**, which had IC_{50} values lower than 20 μM, were evaluated for their ability to inhibit TOP1 and TOP2α. The results are shown in Figure 2.

Figure 2.

Compound **12** had inhibitory activity against TOP2α, and compound **17** slightly inhibited TOP1 and intensely inhibited TOP2α. Additionally, the data presented in Figure 2B showed that compound **17** and VP-16 are almost equal active in inhibiting TOP2α activity.

*2.4. Compound **17** mechanism of action*

To study the effect of compound **17** on TOP2α-mediated DNA cleavage, circular supercoiled plasmid (SC) DNA was used as the substrate in an inhibition model assay to investigate the mode of inhibition; this assay was used in our previous work [13]. The results indicated that compound **17** was a TOP suppressor but not a poison (data not shown).

Figure 3.

2.5. DOCKING

In our previous studies we found that compound **X3** inhibited TOP1 and TOP2α, and we found compound **17** only inhibited TOP2α in this study. So, in order to find the binding site of these compounds to TOP, molecular docking was used to explore the binding of compounds **X3** and **17** to

TOP1 and TOP2α (Figure 3). The main difference was that **X3** could form hydrogen bonds with the TOP1 residues GLU-356 and ASN-722, whereas **17** could form hydrogen bonds with TOP1 residue ASP-533 (Figure 3A). For TOP2α, compound **X3** could form hydrogen bonds with residue ASP-541, whereas **17** could form hydrogen bonds with residues ASP-541 and DG1-10 (Figure 3B). These results were consistent with the TOP inhibition findings.

2.6. 3D-QSAR models and statistics

3D-QSAR is used to correlate compound activity with the interaction fields surrounding the compounds. All compounds, based on minimum energy conformers, were aligned using a terphenyl nucleus as a template. In CoMFA and CoMSIA, partial least-squares (PLS) regression is used to derive and statistically validate models [16].

The 3D-QSAR models were evaluated based on the cross-validated correlation coefficient (q^2), non-cross-validated correlation coefficient (r^2), standard error of estimate (SEE), *F* test value, and evaluation of the model with a test set (r^2_{pred}). The statistical results listed in Table 2 indicate that the CoMFA and CoMSIA models built upon this set of compounds were statistically reliable.

Table 2.

CoMFA and CoMSIA analysis of the statistical parameters indicated that q^2 = 0.605 and 0.622 for the best main fraction of 4 and 5; typically, a representation model with $q^2 > 0.5$ has good prediction ability. Additionally, r^2 = 0.998 and 0.994, SEE was 0.030 and 0.050, and F = 960.9 and 242.5.

The training set consisted of 13 compounds, and their pIC_{50}, predicted values and residual values are presented in Table 3.

Table 3.

2.7. External validation of CoMFA and CoMSIA models

The predictive ability of the CoMFA and CoMSIA models was assessed using a test set of 5 internal molecules (compounds **1**, **2**, **7**, **9**, and **10**) and 5 external molecules (compounds C**1**-**5**, Figure 4), which are shown in Table 4.

Figure 4.

Table 4.

The predictive correlation coefficient r^2_{pred} (test set) was 0.742 and 0.660 for the CoMFA and CoMSIA models, respectively (Table 2). The correlation between the predicted activities and the experimental activities is depicted in Figure 5.

Figure 5.

2.8. Analysis of 3D-QSAR contour maps

The coefficient × standard deviation (coeff*stddev) contour maps of the 3D-QSAR models for the CoMFA and CoMSIA models had good consistency in the electrostatic fields (Figure 6A and B). We observed that electrostatic groups were acceptable and steric substitutions were unacceptable. These results were similar to the DOCK results.

The coeff*stddev maps suggest regions in the model space where adding steric bulk or changing the electrostatic charge at specific loci in the core molecule should increase (or decrease) target activity.[14, 15] Briefly, the green and yellow contours represent favorable and unfavorable steric substitutions, respectively, whereas the red and blue contours represent a favorable effect from *more* electronegative and *more* electropositive substitutions, respectively.

Figure 6.

3. Discussion

In conclusion, we present a simple and rapid protocol for terphenyl synthesis. All of the synthesized compounds were evaluated in MDA-MB-435 cells, and compound **17** displayed the highest cytotoxicity. The TOP2α inhibitory test and docking study of compound **17** suggested that the phenolic hydroxyl group was important for potency. We used CoMFA and CoMSIA to describe the quantitative chemical-biological relationship of terphenyl TOP2α inhibition for the first time. High quantitative correlations were obtained with good results, as evidenced by the high q^2 and r^2 values.

Additionally, the high r^2_{pred} value indicated high predictive power for the activities of untested compounds.

Overall, the current study investigated the anticancer activities and TOP2α inhibition activities of novel variations of *p*-terphenyl derivatives. The antitumor and TOP2α inhibition activities of compound **17**, combined with the results of the DOCK and 3D-QSAR analyses, demonstrated that the ortho-phenolic hydroxyl of ring A was the key group for compound activity. These results provide insight into the key contributions for functional groups of these molecules, which could be used to develop novel synthetic candidates that inhibit TOP2α.

4. Experimental section

4.1. Chemistry

4.1.1. Chemical Syntheses: General Methods

All melting points were determined on a micro melting point apparatus and were uncorrected. ^{1}H-NMR and ^{13}C-NMR spectra were obtained on a *Brucker* Avance-600 NMR spectrometer or an *Inova*-600 NMR spectrometer in the indicated solvents. Chemical shifts are expressed in ppm (δ units) relative to the TMS signal as an internal reference. TLC was performed on Silica Gel GF254 and spots were visualized by iodine vapor or by UV light irradiation (254 nm). Flash column chromatography was performed on a column packed with Silica Gel 60 (200-300 mesh). Solvents were reagent grade and, when necessary, they were purified and dried using standard methods. The concentration of the reaction solutions was performed using a rotary evaporator at reduced pressure. The purity of the product (> 95%) was assessed by reversed-phase HPLC using an Agilent 1200 series and an analytical C18 column using 50% MeOH as solvent system and a flow rate of 1 mL/min with detection wavelength at 254 nm.

4.1.2. General Parallel Procedure a (Scheme 1-4.)

The appropriate bromo derivatives (1 eq.), appropriate phenyl boronic acids (1.5 eq.) and $KF{\cdot}2H_2O$ (3.0 eq.) were dissolved in dioxane and the three resulting mixtures were deoxygenated with

a stream of N_2. After 10 min, $PdCl_2$(dppf) (0.05 eq.) was added, and each mixture was brought to reflux and stirred under N_2 for 5–22 h until the reaction was complete, followed by detection using TLC. Then, each solution was cooled to room temperature. Next, each solution was poured into a mixture of H_2O and ethyl acetate, and the two phases were separated. The aqueous layer was washed with ethyl acetate, and the organic phases were combined and washed with brine. The ethyl acetate layer was dried over anhydrous sodium sulfate and evaporated to dryness under reduced pressure. Each crude product was purified via chromatography or Sephadex LH-20.

4.1.3. General Parallel Procedure b (Scheme 1-4.)

The corresponding compounds (1 eq.) were added to CH_2Cl_2. Then, BBr_3 (3 eq.) was added to each solution and the resulting reaction mixtures were allowed to warm to room temperature for 20 h and treated as follows: Each solution was poured into ice water, followed by warming to ambient temperature, after which each solution was washed twice with ethyl acetate. The combined organic layer was dried over anhydrous sodium sulfate and evaporated to dryness under reduced pressure.[17] The purification of each crude product yielded the corresponding derivatives.

4.1.4. General Parallel Procedure c (Scheme 1-4.)

The corresponding compounds (1 eq.) were added to 50% MeOH. Then, KOH (1.1 eq.) was added to each solution and refluxed for 1 h. Then, each mixture was cooled to room temperature and treated using standard methods.

4.1.5. General Parallel Procedure d (Scheme 1-4.)

The appropriate bromo derivatives (1 eq.) and 4,4,4',4',5,5,5',5'-octamethyl-2,2'-bi (1,3,2-dioxaborolane) (1.1 eq.) and KAc (3.0 eq.) were dissolved in dioxane, and the three resulting mixtures were deoxygenated under a stream of N_2. After 10 min, $PdCl_2$(dppf) (0.05 eq.) was added, and each mixture was brought to 60-80°C and stirred under N_2 for 2–4 h until the reaction was complete, followed by detection using TLC. After the reaction was finished, without further treatment the crude product was subjected to a second coupling reaction.

4.1.6. General Parallel Procedure e (Scheme 1-4.)

The appropriate bromo derivatives (1 eq.), appropriate phenyl boronic acids (3 eq.) and KF (3.0 eq.) were respectively dissolved in dioxane, and the three resulting mixtures were deoxygenated under a stream of N_2. After 10 min, $PdCl_2$(dppf) (0.05 eq.) was added, and each mixture was brought to reflux and was stirred under N_2 for 5–22 h until the reaction was complete, followed by detection using TLC. Then, each solution was cooled to room temperature. Next, each solution was poured into a mixture of H_2O and ethyl acetate and the two phases were separated. The aqueous layer was washed with ethyl acetate, and the organic phases were combined and then washed with brine. The ethyl acetate layer was dried over anhydrous sodium sulfate and evaporated to dryness under reduced pressure. Each crude product was purified by chromatography using petroleum ether/ethyl acetate, which yielded the corresponding derivatives.

*4.1.7. 4,4''-dihydroxy-2',3'-dimethoxy [1,1':4',1''-terphenyl]-3-carboxylic acid methyl ester (**1**)*

The resulting residue was purified by silica gel chromatography (10/1 PET/EtOAc) to afford the desired product as a white solid (55.6 %): mp 178-180 °C; ^{1}H NMR (600 MHz, $(CD_3)_2CO$, rt) δ 10.80 (s, 1H, OH), 8.43 (s, 1H, OH), 8.08 (s, 1H, H2) 7.79 (d, *J* = 8.4 Hz, 1H, H6) 7.46 (d, *J* = 7.2 Hz, 2H, H2", H6"), 7.16(s, 2H, H5', H6'), 7.07 (d, *J* = 8.4 Hz, 1H, H5) 6.94 (d, *J* = 7.8 Hz, 2H, H3", H5"), 4.01 (s, 3H, $COOCH_3$), 3.70 (s, 3H, OCH_3), 3.67 (s, 3H, OCH_3) ^{13}C NMR (150 MHz, $(CD_3)_2CO$, rt) δ 170.5 (CO), 160.7 (C4), 156.9 (C4"), 151.07 (C2'), 151.06 (C3'),136.7 (C6), 135.5 (C2), 133.3 (C1"), 130.2 (C2"), 130.2 (C6"), 130.1 (C1), 129.3 (C1'), 129.1 (C4'), 125.3 (C6'), 124.9 (C5'), 117.2 (C5), 115.1 (C3"), 115.1 (C5"), 112.1 (C3), 60.0 ($COO\mathbf{C}H_3$), 59.8 ($O\mathbf{C}H_3$), 52.1 ($O\mathbf{C}H_3$); HRMS (ESI) *m/z* $[M+H]^+$ Calcd. for $C_{22}H_{21}O_6$: 381.1338, Found: 381.1359.

*4.1.8. 3,4''-dihydroxy-2',3'-dimethoxy [1,1':4',1''-terphenyl]-4- carboxylic acid methyl ester (**2**)*

The resulting residue was purified by silica gel chromatography (10/1 PET/EtOAc) to afford the desired product as a white solid (62.1 %): mp 140-142 °C; ^{1}H NMR (600 MHz, $(CD_3)_2CO$, rt) δ 10.79 (s, 1H, OH), 8.45 (s, 1H, OH), 7.91 (d, *J* = 8.4 Hz, 1H, H2) 7.47 (d, *J* = 8.4 Hz, 2H, H2", H6"),

7.18~7.21 (brs, 4H, H5, H5', H6, H6'), 6.95 (d, *J* = 8.4 Hz, 2H, H3", H5") 4.01 (s, 3H, COOC**H**$_3$), 3.73 (s, 3H, OCH_3), 3.67 (s, 3H, OCH_3). ^{13}C NMR (150 MHz, $(CD_3)_2CO$, rt) δ 170.4 (CO), 161.3 (C3), 157.0 (C4"), 151.3 (C2'), 151.1 (C3'), 146.0 (C1), 136.5 (C1"), 133.2 (C1'), 130.2 (C2"), 130.2 (C6"), 129.5 (C5), 128.9 (C4'), 125.3 (C6'), 125.1 (C5'), 120.4 (C6), 117.6 (C2), 115.1 (C3"), 115.1 (C5"), 110.9 (C4), 60.3 (COO**C**H_3), 59.8 (OCH_3), 52.0 (OCH_3) ; HRMS (ESI) *m/z* $[M+H]^+$ Calcd. for $C_{22}H_{21}O_6$: 381.1338, Found: 381.1334.

*4.1.9. 4,4''-dihydroxy-2',3'-dimethoxy [1,1':4',1''-terphenyl]- 3-carboxylic acid (**3**)*

The resulting residue was purified by sephadex LH-20 chromatography (1/1 MeOH/Acetone) to afford the desired product as a grey white solid(58.4 %): mp 250-253 °C; ^{1}H NMR (600 MHz, $(CD_3)_2CO$, rt) δ 11.18 (s, 1H, OH), 8.50 (s, 1H, OH), 8.15 (s, 1H, H2), 7.80 (d, *J* = 9 Hz, 1H, H6), 7.47(d, *J* = 7.8 Hz, 2H, H2", H6"), 7.19 (d, *J* = 9.6 Hz, 1H, H5'), 7.17 (d, *J* = 9.6 Hz, 1H, H6'), 7.07(d, *J* = 9 Hz, 1H, H5), 6.95 (d, *J* = 7.2 Hz, 2H, H3", H5"), 3.72 (s, 3H, OCH), 3.68 (s, 3H, OCH); ^{13}C NMR (150 MHz, $(CD_3)_2CO$, rt) δ 171.8 (CO), 161.3 (C4), 156.8 (C4"), 151.1 (C2'), 151.1 (C3'), 136.8 (C6), 135.4 (C1"), 133.3 (C1), 130.7 (C2), 130.2 (C2"), 130.2 (C6"), 129.2 (C4'), 129.1 (C1'), 125.3 (C5'), 124.9 (C6'), 117.1 (C5), 115.0 (C3"), 115.0 (C5"), 112.0 (C3), 60.0 (OCH_3), 59.8 (OCH_3); HRMS (ESI) *m/z* $[M+H]^+$ Calcd. for $C_{21}H_{19}O_6$: 367.1182, Found: 367.1180.

*4.1.10. 3,4''-dihydroxy-2',3'-dimethoxy [1,1':4',1''-terphenyl]- 4-carboxylic acid (**4**)*

The resulting residue was purified by sephadex LH-20 chromatography (1/1 MeOH/Acetone) to afford the desired product as a grey white solid (76.3 %): mp 244-247 °C; ^{1}H NMR (600 MHz, $(CD_3)_2CO$, rt) δ 7.97 (d, *J* = 7.8 Hz, 1H, H6), 7.48 (d, *J* = 7.8 Hz, 2H, H2", H6"), 7.19~7.22 (m, 4H, H2, H3', H5, H5'), 6.95 (d, *J* = 7.2 Hz, 2H, H3", H5"), 3.74 (s, 3H, OCH), 3.68 (s, 3H, OCH); ^{13}C NMR (150 MHz, $(CD_3)_2CO$, rt) δ 171.6 (CO), 161.7 (C3), 156.9 (C4"), 151.3 (C3'), 151.1 (C2'), 146.0 (C1), 136.4 (C1"), 133.2 (C4'), 130.2 (C2"), 130.2 (C6"), 130.0 (C5), 128.9 (C1'), 125.3 (C5'), 125.1 (C6'), 120.3 (C6), 117.5 (C2), 115.0 (C3"), 115.0 (C5"), 110.8 (C4); HRMS (ESI) *m/z* $[M-H]^-$ Calcd. for $C_{21}H_{17}O_6$: 365.1025, Found: 365.1029.

*4.1.11. 2',3',4,4''-tetrahydroxy [1,1':4',1''-terphenyl]-3-carboxylic acid (**5**)*

The reaction maxture was poured into ice water, and the resulting precipitate was filtered to afford the desired product as a grey white solid (63.1%): mp > 260 °C; ^{1}H NMR (600 MHz, $(CD_3)_2CO$, rt) δ 8.20 (s, 1H, H2), 7.83 (d, *J* = 8.4 Hz, 1H, H6), 7.46 (d, *J* = 7.8 Hz, 2H, H2", H6"), 7.05 (d, *J* = 8.4 Hz, 1H, H5), 6.91~6.93 (3H, H3", H5", H6') 6.88 (d, *J* = 7.8 Hz, 1H, H5'); ^{13}C NMR (150 MHz, $(CD_3)_2CO$, rt) δ 171.7 (CO), 160.9 (C4), 156.5 (C4"), 142.7 (C2'), 142.2 (C3'), 136.9 (C6), 130.7 (C2), 130.3 (C2"), 130.3 (C6"), 129.6 (C1"), 129.3 (C1), 128.2 (C4'), 126.1 (C1'), 121.2 (C5'), 120.9 (C6'), 117.0 (C5), 115.1 (C3"), 115.1 (C5"), 111.9 (C3); HRMS (ESI) *m/z* $[M-H]^-$ Calcd. for $C_{19}H_{13}O_6$: 337.0712, Found: 337.0704.

*4.1.12. 2',3,3',4''-tetrahydroxy [1,1':4',1''-terphenyl]-4-carboxylic acid (**6**)*

The resulting residue was purified by sephadex LH-20 chromatography (1/1 MeOH/Acetone) to afford the desired product as a grey white solid (85.7 %): mp > 260 °C; ^{1}H NMR (600 MHz, $(CD_3)_2CO$, rt) δ 7.95 (d, *J* = 8.4 Hz, 1H, H6), 7.46 (d, *J* = 7.8 Hz, 2H, H2", H6"), 7.28 (s, 1H, H2), 7.25 (d, *J* = 8.4 Hz, 1H, H5), 6.98 (d, *J* = 8.4 Hz, 1H, H5'), 6.93 (d, *J* = 7.8 Hz, 2H, H3", H5"), 6.89 (d, *J* = 8.4 Hz, 1H, H6'); ^{13}C NMR (150 MHz, $(CD_3)_2CO$, rt) δ 171.7 (CO), 161.9 (C3), 156.8 (C4"), 146.5 (C1), 143.2 (C3'), 142.4 (C2'), 130.3 (C2"), 130.3 (C6"), 130.1 (C5), 129.3 (C4'), 129.1 (C1'), 125.9 (C1"), 121.2 (C5'), 121.0 (C6'), 120.2 (C6), 117.5 (C2), 115.2 (C3"), 115.2 (C5"), 110.5 (C4); HRMS (ESI) *m/z* $[M-H]^-$ Calcd. for $C_{19}H_{13}O_6$: 337.0712, Found: 337.0713.

*4.1.13. 2',3,3',4-tetramethoxy[1,1':4',1''-terphenyl] -4''-carboxylic acid (**7**)*

The resulting residue was purified by silica gel chromatography (10/1 PET/EtOAc) to afford the desired product as a white solid (21.1 %): mp 241-243 °C; ^{1}H NMR (600 MHz, DMSO-*d6*, rt) δ 13.00 (s, 1H, COOH), 8.04 (d, *J* = 8.4 Hz, 2H, H2", H6"), 7.68 (d, *J* = 8.4 Hz, 2H, H3", H5") 7.24 (d, *J* = 8.4 Hz, 1H, H6'), 7.21 (d, *J* = 7.8 Hz, 1H, H5'), 7.16 (s, 1H, H2), 7.12 (d, *J* = 8.4 Hz, 1H, H6), 7.06 (d, *J* = 8.4 Hz, 1H, H5), 3.82 (s, 6H, OC**H**$_3$), 3.66 (s, 3H, OC**H**$_3$), 3.65 (s, 3H, OC**H**$_3$); ^{13}C NMR (150 MHz, DMSO-*d6*, rt) δ 167.7 (CO), 151.2 (C3), 151.1 (C4), 148.8 (C2'), 148.75 (C6'), 142.5 (C1"), 136.0 (C1), 133.9 (C4"), 130.2 (C1'), 129.9 (C4'), 129.8 (C2"), 129.8 (C6"), 129.6 (C3"), 129.6 (C5"), 125.9 (C6), 125.7 (C6'), 121.6 (C5'), 113.1 (C2), 112.1 (C5), 61.1 (O**C**H$_3$), 60.9 (O**C**H$_3$), 56.0 (O**C**H$_3$), 56.0

(O**C**H_3); HRMS (ESI) *m/z* $[M+H]^+$ Calcd. for $C_{23}H_{23}O_6$: Calcd. for $C_{23}H_{23}O_6$: 395.1495, Found: 395.1485.

*4.1.14. 2',3,3',4-tetrahydroxy [1,1':4',1''-terphenyl] -4''-carboxylic acid (**8**)*

The resulting residue was purified by sephadex LH-20 chromatography (1/1 MeOH/Acetone) to afford the desired product as a white solid (73.3 %): mp > 260 °C; ^{1}H NMR (600 MHz, CD_3OD, rt) δ 8.08 (d, *J* = 7.2 Hz, 2H, H2", H6"), 7.75 (d, *J* = 7.8 Hz, 2H, H3", H5"), 7.09 (s, 1H, H2), 6.95 (d, *J* = 7.8 Hz, 1H, H6), 6.90 (d, *J* = 7.8 Hz, 1H, H5'), 6.86 (d, *J* = 7.2 Hz, 1H, H6'), 6.85 (d, *J* = 6.6 Hz, 1H, H5); ^{13}C NMR (150 MHz, CD_3OD, rt) δ 168.6 (CO), 144.7 (C4), 144.4 (C3), 143.8 (C3'), 143.2 (C2'), 142.3 (C1"), 130.0 (C1), 129.4 (C4"), 129.2 (C2"), 129.2 (C6"), 128.8 (C3"), 128.8 (C5"), 128.4 (C4'), 126.2 (C1'), 121.0 (C5'), 120.9 (C6'), 120.4 (C6), 116.0 (C2), 114.9 (C5); HRMS (ESI) *m/z* $[M-H]^-$ Calcd. for $C_{19}H_{13}O_6$: 337.0712, Found: 337.0718.

*4.1.15. 3,3''-dinitro-2',3'-dimethoxy -4,4''-dihydroxy [1,1':4',1''-terphenyl] (**9**)*

The resulting residue was purified by silica gel chromatography (10/1 PET/EtOAc) to afford the desired product as a grey yellow solid (43.6 %): mp 175-177 °C; ^{1}H NMR (600 MHz, $CDCl_3$, rt) δ 10.67 (s, 2H, OH), 8.36 (s, 2H, H2, H2"), 7.88 (d, *J* = 8.4 Hz, 2H, H6, H6"), 7.26 (d, *J* = 9 Hz, 2H, H5, H5"), 7.19 (s, 2H, H5', H6'); ^{13}C NMR (150 MHz, $CDCl_3$, rt) δ 154.4 (C4), 154.4 (C4"), 151.1 (C2'), 151.1 (C3'), 138.7 (C6), 138.7 (C6"), 133.5 (C3), 133.5 (C3"), 133.4 (C1), 133.4 (C1"), 130.1 (C1'), 130.1 (C4'), 125.2 (C2), 125.2 (C2"), 125.1 (C5'), 125.1 (C6'), 119.8 (C5), 119.8 (C5"); HRMS (ESI) *m/z* $[M-H]^-$ Calcd. for $C_{20}H_{15}N_2O_8$: 411.0828, Found: 411.0832.

*4.1.16. 4,4''-dihydroxy-2',3'-diethoxy [1,1':4',1''-terphenyl] (**10**)*

The resulting residue was purified by silica gel chromatography (5/1 PET/EtOAc) to afford the product as a white solid then was purified by sephadex LH-20 chromatography (MeOH) to afford the desired product as a white solid (64.2 %): mp 105-107 °C; ^{1}H NMR (600 MHz, CD3OD, rt) δ7.43(d, *J* = 8.4 Hz, 4H, H2, H2", H6, H6"), 7.09(s, 2H, H5', H6'), 6.86(d, *J* = 8.4 Hz, 4H, H3, H3", H5, H5"), 3.84(q, *J* = 7.2 Hz, 4H, OC**H**$_2$), 1.18(t, *J* = 7.2 Hz, 6H, C**H**$_3$). ^{13}C NMR (150 MHz, CD3OD, rt) δ 156.4 (C4), 156.4 (C4"), 150.0 (C2'), 150.0 (C3'), 135.0 (C1), 135.0 (C1"), 130.0 (C2), 130.0 (C2"), 130.0

(C6), 130.0 (C6”), 129.5 (C1’), 129.5 (C4’), 124.9 (C5’), 124.9 (C6’), 114.5 (C3), 114.5 (C3”), 114.5 (C5), 114.5 (C5”), 68.4 (O**C**H_2), 68.4 (O**C**H_2), 14.6 (**C**H_3), 14.6 (**C**H_3); HRMS (ESI) *m/z* $[M-H]^-$ Calcd. for $C_{22}H_{21}O_4$: 349.1440, Found: 349.1455.

*4.1.17. 3,3’’,4,4’’-tetramethoxy-2’,3’-diethoxy [1,1’:4’,1’’-terphenyl] (**11**)*

The resulting residue was purified by silica gel chromatography (10/1 PET/EtOAc) to afford the desired product as a withe solid (31.2 %): mp 101-103 °C. ^{1}H NMR (600 MHz, CDCl3, rt) δ 7.26 (d, *J* = 1.8 Hz, 2H, H2, H2”), 7.16 (s, 2H, H5’, H6’), 7.15 (dd, *J* = 8.4, 1.8 Hz, 2H, H6, H6”), 6.96 (d, *J* = 8.4 Hz, 2H, H5, H5”) , 3.96 (s, 6H, O**C**H_3), 3.95 (s, 6H, O**C**H_3), 3.85 (q, *J* = 7.2 Hz,4H, OC**H**$_2$), 1.23 (t,6H, CH_2C**H**$_3$). ^{13}C NMR (150 MHz, CDCl3, rt) δ 150.3 (C3), 150.3 (C3”), 148.3 (C4), 148.3 (C4”), 148.2 (C2’), 148.2 (C3’), 135.1 (C1), 135.1 (C1”), 131.1 (C1’), 131.1 (C4’), 125.3 (C6), 125.3 (C6”), 121.4 (C5’), 121.4 (C6’), 112.6 (C2), 112.6 (C2”), 110.8 (C5), 110.8 (C5”), 69.0 (O**C**H_2CH_3), 69.0 (O**C**H_2CH_3), 55.9 (O**C**H_3), 55.9 (O**C**H_3), 55.9 (O**C**H_3), 55.9 (O**C**H_3), 15.9 (OCH_2**C**H_3), 15.9 (OCH_2**C**H_3); HRMS (ESI) *m/z* $[M+H]^+$ Calcd. for $C_{26}H_{31}O_6$: 439.2120, Found: 439.2119.

*4.1.18. 4,4’’-dihydroxy-2’,3’-dimethoxy [1,1’:4’,1’’-terphenyl] (**12**)*

The resulting residue was purified by silica gel chromatography (10/1 PET/EtOAc) to afford the product as a white solid then was purified by sephadex LH-20 chromatography (MeOH) to afford the desired product as a white solid (41.6 %): mp 178-180 °C; ^{1}H NMR (600 MHz, CD3OD, rt) δ 7.42(d, *J* = 8.4 Hz, 4H, H2, H2”, H6, H6”), 7.10(s, 2H, H5’ H6’), 6.86(d, *J* = 8.4 Hz, 4H, H3, H3”, H5, H5”), 3.65(s, 6H, OC**H**$_3$). ^{13}C NMR (150 MHz, CD3OD, rt) δ 156.5 (C4), 156.5 (C4”), 150.8 (C2’), 150.8 (C3’), 134.7 (C1), 134.7 (C1”), 129.9 (C2), 129.9 (C2”), 129.9 (C6), 129.9 (C6”), 129.3 (C1’), 129.3 (C4’), 125.0 (C5’), 125.0 (C6’), 114.6 (C3), 114.6 (C3”), 114.6 (C5), 114.6 (C5”), 59.6 (O**C**H_3), 59.6 (O**C**H_3); HRMS (ESI) *m/z* $[M-H]^-$ Calcd. for $C_{20}H_{17}O_4$: 321.1127, Found: 321.1145.

*4.1.19. 4,4’’-dimethoxy-2’,3’-diacetoxy[1,1’:4’,1’’-terphenyl] (**13**)*

The resulting residue was purified by silica gel chromatography (5/1 PET/EtOAc) to afford the desired product as a withe solid (28.9 %): mp 178-180 °C; ^{1}H NMR (600 MHz, CDCl3, rt) δ 7.43(d, *J* = 7.8 Hz, 4H, H2, H2”, H6, H6”), 7.35(s, 2H, H5’ H6’), 6.98(d, *J* = 7.8 Hz, 4H, H3, H3”, H5, H5”),

3.87(s, 4H, OC**H**$_3$) , 2.14(S, 6H OCOC**H**$_3$). ^{13}C NMR (150 MHz, CDCl3, rt) δ 168.3 (CO), 168.3 (CO), 159.2 (C4), 159.2 (C4”), 140.4 (C2’), 140.4 (C3’), 134.9 (C1’), 134.9 (C4’), 129.9 (C2), 129.9 (C2”), 129.9 (C6), 129.9 (C6”), 129.2 (C1), 129.2 (C1”), 127.8 (C5’), 127.8 (C6’), 113.9 (C3), 113.9 (C3”), 113.9 (C5), 113.9 (C5”), 55.3 (O**C**H$_3$), 55.3 (O**C**H$_3$), 20.5 (CO**C**H$_3$), 20.5 (CO**C**H$_3$) HRMS (ESI) *m/z* $[M+Na]^+$ Calcd. for $C_{24}H_{22}O_6Na$: 429.1314, Found: 429.1302.

*4.1.20. 3,3’’,4,4’’-tetramethoxy-2’,3’-diacetoxy[1,1’:4’,1’’-terphenyl] (**14**)*

The resulting residue was purified by silica gel chromatography (3/1 PET/EtOAc) to afford the desired product as a withe solid (19.4 %): mp 196-197 °C; ^{1}H NMR (600 MHz, CDCl3, rt) δ 7.38(s, 2H, H5’, H6’), 7.05(d, *J* = 8.4 Hz, 2H, H6, H6”), 7.02(s, 2H, H2, H2”), 6.95(d, *J* = 7.8 Hz, 2H, H5, H5”) , 3.95(s, 6H, OC**H**$_3$), 3.92(s, 6H, OC**H**$_3$), 2.15(s, 6H, COC**H**$_3$). 13C NMR (150 MHz, CDCl3, rt) δ 168.3 (CO), 168.3 (CO), 148.7 (C3), 148.7 (C3”), 148.6 (C4), 148.6 (C4”), 140.4 (C2’), 140.4 (C3’), 135.2 (C1’), 135.2 (C4’), 129.5 (C1), 129.5 (C1”), 127.9 (C5’), 127.9 (C6’), 121.2 (C6), 121.2 (C6”), 111.9 (C2), 111.9 (C2”), 111.1 (C5), 111.1 (C5”), 55.9 (O**C**H$_3$), 55.9 (O**C**H$_3$), 55.9 (O**C**H$_3$), 55.9 (O**C**H$_3$), 20.6 (CO**C**H$_3$), 20.6 (CO**C**H$_3$) HRMS (ESI) *m/z* $[M+Na]^+$ Calcd. for $C_{26}H_{26}O_8Na$: 489.1526, Found: 489.1511.

*4.1.21. [1,1’:4’,1”-Terphenyl]- 2’,3’,4,4’’-tetraol (**15**)*

The resulting residue was purified by recrystallization in acetone to afford the desired product as a withe solid (52.1%): mp > 260 °C; ^{1}H NMR (600 MHz, $(CD_3)_2CO$, rt) δ 7.46 (d, *J* = 7.8 Hz, 4H, H2, H2”, H6, H6”), 6.91 (d, *J* = 7.8 Hz, 4H, H3, H3”, H5, H5”), 6.84 (s, 2H, H5’, H6’); ^{13}C NMR (150 MHz, $(CD_3)_2CO$, rt) δ 156.4 (C4), 156.4 (C4”), 142.3 (C2’), 142.3 (C3’), 130.2 (C2), 130.2 (C2”), 130.2 (C6), 130.2 (C6”), 129.6 (C1), 129.6 (C1”), 127.4 (C1’), 127.4 (C4’), 121.0 (C5’), 121.0 (C6’), 115.0 (C3), 115.0 (C3”), 115.0 (C5), 115.0 (C5”); HRMS (ESI) *m/z* $[M-H]^-$ Calcd. for $C_{18}H_{13}O_4$: 293.0814, Found: 293.0809.

*4.1.22. 2’,3,3’,3’’,4,4’’-hexamethoxy-[1,1’:4’,1’’-terphenyl] (**16**)*

The resulting residue was purified by silica gel chromatography (15/1 PET/EtOAc) to afford the desired product as a withe solid (12.3 %): mp 130-132 °C; ^{1}H NMR (600 MHz, $(CD_3)_2CO$, rt) δ 7.22 (s,

2H, H5', H6'), 7.17 (s, 2H, H2, H2"), 7.14 (d, *J* = 8.4 Hz, 2H, H6, H6") 7.03 (d, *J* = 8.4 Hz, 2H, H5, H5"), 3.88 (s, 6H, OCH_3), 3.87 (s, 6H, OCH_3), 3.70 (s, 6H, OCH_3) ^{13}C NMR (150 MHz, $(CD_3)_2CO$, rt) δ 151.1 (C3), 151.1 (C3"),149.1 (C2'), 149.1 (C3'), 148.9 (C4), 148.9 (C4"), 134.8 (C1), 134.8 (C1"), 130.8 (C1'), 130.8 (C4'), 125.2 (C6), 125.2 (C6"), 121.4 (C5'), 121.4 (C6'), 113.2 (C2), 113.2 (C2"), 111.6 (C5), 111.6 (C5"), 59.9 (O**C**H_3), 59.9 (O**C**H_3), 55.3 (O**C**H_3), 55.3 (O**C**H_3), 55.2 (O**C**H_3), 55.2 (O**C**H_3) ; HRMS (ESI) *m/z* $[M+H]^+$ Calcd. for $C_{24}H_{27}O_6$: 411.1808, Found: 411.1814.

*4.1.23. [1,1':4',1"-Terphenyl]-2',3,3',3'',4,4''-hexaol (**17**)*

The resulting residue was purified by sephadex LH-20 chromatography (1/1 MeOH/CH_2Cl_2) to afford the desired product as a grey white solid (80.0 %): mp > 260 °C; ^1H NMR (600 MHz, $(CD_3)_2CO$, rt) δ 7.98 (s, 2H, OH), 7.91 (s, 2H, OH), 7.43 (s, 2H, OH), 7.13 (s, 2H, H5',H6'), 6.95 (d, *J* = 8.4 Hz, 2H, H5, H5"), 6.88 (d, *J* = 8.4 Hz, 2H, H6, H6"), 6.81 (s, 2H, H3, H3"); ^{13}C NMR (150 MHz, $(CD_3)_2CO$, rt) δ 144.7 (C4), 144.7 (C4"), 144.3 (C3), 144.3 (C3"), 142.3 (C2'), 142.3 (C3'), 130.2 (C1), 130.2 (C1"), 127.4 (C1'), 127.4 (C4'), 120.8 (C6), 120.8 (C6"), 120.7 (C5'), 120.7 (C6'), 116.3 (C2), 116.3 (C2"), 115.2 (C6), 115.2 (C6"); HRMS (ESI) *m/z* $[M-H]^-$ Calcd. for $C_{18}H_{13}O_6$: 325.0712, Found: 325.0708.

*4.1.24. dimethyl biphenyl-4,4'-dicarboxylate (**18**)*

The resulting residue was purified by silica gel chromatography (5/1 PET/EtOAc) to afford the desired product as a withe solid (29.7 %): mp 108-110 °C; ^1H NMR (600 MHz, $CDCl_3$, rt) δ 8.15 (d, *J* = 8.4 Hz, 4H, H3, H3', H5, H5'), 7.71 (d, *J* = 8.4 Hz, 4H, H2, H2', H6, H6'), 3.97 (s, 6H, OCH_3). ^{13}C NMR (150 MHz, $CDCl_3$, rt) δ 166.8 (CO), 166.8 (CO), 144.3 (C1), 144.3 (C1'), 130.2 (C2), 130.2 (C2'), 130.2 (C6), 130.2 (C6'), 129.7 (C4), 129.7 (C4'), 127.2 (C3), 127.2 (C3'), 127.2 (C5), 127.2 (C5'), 52.2 (O**C**H_3), 52.2 (O**C**H_3) ; HRMS (ESI) *m/z* $[M+H]^+$ Calcd. for $C_{16}H_{15}O_4$: 271.0970, Found: 271.0977.

*4.1.25. 2,3,3',4'-tetramethoxybiphenyl (**19**)*

The resulting residue was purified by silica gel chromatography (15/1 PET/EtOAc) to afford the desired product as a yellow oil (10.4 %): ^1H NMR (600 MHz, $(CD_3)_2CO$, rt) δ 7.15 (s, 1H, H2),

7.06~7.11 (m, 2H, H6, H6'), 6.99~7.02 (t, 2H, H5, H5') 6.94 (d, *J* = 7.8 Hz, 1H, H4'), 3.89 (s, 3H), 3.86 (s, 6H), 3.61 (s, 3H) ^{13}C NMR (150 MHz, $(CD_3)_2CO$, rt) δ 153.4 (C2'), 148.9 (C3'), 148.8 (C3), 146.6 (C4), 135.5 (C1), 131.1 (C1'), 123.9 (C6'), 122.2 (C5'), 121.4 (C6), 113.4 (C5), 111.6 (C2), 111.6 (C4'), 59.6 (O**C**H_3), 55.3 (O**C**H_3), 55.2 (O**C**H_3), 55.19 (O**C**H_3).

*4.1.26. 3,3'-dinitro -4,4''-dihydroxy diphenyl (**20**)*

The resulting residue was purified by silica gel chromatography (15/1 PET/EtOAc) to afford the desired product as a yellow solid (25.5 %): mp > 260 °C; ^{1}H NMR (600 MHz, DMSO-*d6*, rt) δ11.16 (s, 2H, OH), 8.15 (s, 2H, H2, H2'), 7.87 (d, *J* = 8.4 Hz, 2H, H6, H6'), 7.20 (d, *J* = 9 Hz, 2H, H5, H5'); ^{13}C NMR (150 MHz, DMSO-*d6*,, rt) δ 151.7 (C4), 151.7 (C4'), 137.9 (C3), 137.9 (C3'), 133.2 (C6), 133.2 (C6'), 129.5 (C1), 129.5 (C1'), 122.9 (C2), 122.9 (C2'), 120.1 (C5), 120.1 (C5').

*4.1.27. methyl 2-hydroxy-5-(4,4,5,5-tetramethyl-1,3,2-dioxaborolan-2-yl)benzoate (**21**)*

The resulting residue was purified by silica gel chromatography (15/1 PET/EtOAc) to afford the desired product as a withe solid (53.3 %): ^{1}H NMR (600 MHz, $CDCl_3$) δ 11.01 (s, 1H), 8.31 (s, 1H), 7.88 (dd, *J* = 7.4, 1.2 Hz, 1H), 6.97 (d, *J* = 7.4 Hz, 1H), 3.95 (s, 3H), 1.34 (s, 12H); ^{13}C NMR (150 MHz, $CDCl_3$) δ 170.7, 164.0, 141.96, 137.3, 117.1, 112.1, 83.8, 77.2, 77.0, 76.8, 52.2, 24.9.

*4.1.28. methyl 2-hydroxy-4-(4,4,5,5-tetramethyl-1,3,2-dioxaborolan-2-yl)benzoate (**22**)*

The crude product was purified by chromatography using petroleum ether/ethyl acetate 30:1 to yield the corresponding derivatives (41.1%). ^{1}H NMR (600 MHz, $CDCl_3$, rt) δ 10.62 (s, 1H), 7.83 (d, *J* = 6.8 Hz, 1H), 7.44 (s, 1H), 7.30 (d, *J* = 6.8 Hz, 1H), 3.97 (s, 3H), 1.37 (s, 12H).

*4.1.29. 4-bromo-2,3,3',4'-tetramethoxybiphenyl (**25**)*

The resulting residue was purified by silica gel chromatography (15/1 PET/EtOAc) to afford the desired product as a withe solid (73.3 %): ^{1}H NMR (600 MHz, Acetone) δ 7.35 (d, *J* = 8.4 Hz, 1H, H6), 7.17 (s, 1H, H2), 7.06~7.09 (2H, H5', H6'), 7.00 (d, *J* = 8.4 Hz, 1H, H5), 3.92 (s, 3H, OCH_3),

3.86 (s, 6H, OCH_3), 3.66 (s, 3H, OCH_3); ^{13}C NMR (150 MHz, Acetone) δ 151.8 (C3'), 151.1 (C2'), 149.2 (C3), 149.1 (C4), 135.9 (C1), 129.8 (C1'), 127.7 (C5'), 126.4 (C6'), 121.4 (C6), 115.7 (C4'), 113.0 (C2), 111.7 (C5), 60.2 (O**C**H_3), 60.17 (O**C**H_3), 55.4 (O**C**H_3), 55.3 (O**C**H_3).

*4.1.30. 1,4-dibromo-2,3-diethoxybenzene (**30**)*

0^0C, 1,2-Benzenediol,3,6-dibromo (360mg), anhydrous potassium carbonate (747mg), anhydrous acetone (3ml), diethyl sulfate (0.71ml). After being stirred overnight, the mixture was quenched with sufficient quantum aqueous ammonia and extracted with ethyl acetate. The aqueous layer was washed with ethyl acetate. The organic phases were combined, washed with brine, dried over anhydrous sodium sulfate and evaporated to dryness under reduced pressure. The crude product was purified by chromatography using petroleum ether/ethyl acetate 20:1 to yield the corresponding derivatives (71.1%). ^1H NMR (600 MHz, $CDCl_3$, rt) δ 7.19(s, 2H), 4.14(q, 4H), 1.44(t, 6H); ^{13}C NMR (150 MHz, $CDCl_3$, rt) δ 151.0, 151.0, 128.5, 128.5, 117.5, 117.5, 69.7, 69.7, 15.7, 15.7.

*4.1.31. 3,6-dibromo-1,2-phenylene diacetate (**31**)*

3,6-dibromobenzene-1,2-diol [13] was acetylated by acetic anhydride gained **31**.

4.2. Biological Assay

4.2.1. In vitro cytotoxicity assays

The cytotoxicity was measured by the MTT assay as described in the literature [18, 19]. The cells plated in the wells of 96-well plates (Falcon, USA) were treated in triplicate with various concentrations of compounds for 72 h in 5% CO_2 incubator at 37°C. After fresh medium being changed, a 20 μL aliquot of MTT solution (5 mg/mL) was added and incubated for 4 h at 37°C. Then, 100 μL of triplex solution (10% SDS, 5% isobutanol, 12 mM HCl) was added to each well and incubated overnight at 37°C. The absorbance of each well was determined by a microplate reader (M-3350, Bio-Rad) with a 590 nm wavelength. Growth inhibition rates were calculated with the following equation:

$$Inhibition\ rate = \frac{OD\ control\ well - OD\ treated\ well}{OD\ control\ well - OD\ blank\ well} \times 100\%$$

4.2.2. DNA gel electrophoresis assay of topoisomerases

Plasmid pBR322 DNA and purified calf thymus DNA TOP1 were purchased from TakaRa Biotechnology (Dalian) Co., Ltd., recombinant human TOP2α was obtained from TopoGENINC (USA). All experiments were done at least in duplicate to confirm the results.

4.2.3. DNA relaxation assay

DNA TOP1 inhibition assay was performed as described previously [20] with minor modifications. The test compounds were dissolved in DMSO at 20 mM as stock solution. The activity of DNA TOP1 was determined by assessing the relaxation of supercoiled DNA pBR322. The mixture of 0.5 μg of plasmid pBR322 DNA and 1 units of TOP1 was incubated without and with the prepared compounds at 37 °C for 30 min in the relaxation buffer (10 mM Tris-HCl (pH 7.9), 150 mM NaCl, 0.1% bovine serum albumin, 1 mM spermidine, 5% glycerol). The reaction in the final volume of 20 μL was terminated by adding 2.5 μL of the stop solution containing 5% sarcosyl, 0.0025% bromophenol blue, and 25% glycerol. DNA samples were then electrophoresed on a 1% agarose gel at 5 V /cm for 2 h with a running buffer of TAE. Gels were stained for 30 min in an aqueous solution of ethidium bromide (0.5 μg/mL) and photographed under UV light.

DNA TOP2α inhibitory activity of compounds was measured as follows [21]. Briefly, the mixture of 0.5 μg of supercoiled pBR322 plasmid DNA and 1 units of TOP2α was incubated without and with the prepared compounds in the assay buffer (10 mM Tris-HCl (pH 7.9) containing 50 mM NaCl, 50 mM KCl, 5 mM $MgCl_2$, 1 mM EDTA, 1 mM ATP, and 15 lg/mL bovine serum albumin) for 30 min at 30 °C. The reaction in a final volume of 20 μL was terminated by the addition of 3 μL of 7 mM EDTA. Reaction products were analyzed on a 1% agarose gel at 5 V /cm for 2 h with a running buffer of TAE. Gels were stained for 30 min in an aqueous solution of ethidium bromide (0.5 μg/mL) and photographed under UV light.

4.3. DOCK

The molecular docking was conducted using AutoDock Vina 1.1.2 [22] an open-source program for doing molecular docking. Compounds **17** and **X3** were ultimately converted to the PDBQT format

using AutoDock Tools 1.5.6 [http:/mgltools.scripps.edu], which is required for AutoDock Vina. The 3-dimensional (3D) structure of TOP1 and TOP2α were downloaded from the Protein Data Bank (PDBID: 1T8I and 4FM9, respectively). Using AutoDock Tools, the PDB (1T8I) structure was converted from a pdb file to a pdbqt file and the search grid was identified as center_x: 21.95, center_y: -4.434, and center_z: 27.801 with dimensions size_x: 16, size_y: 16, and size_z: 16. Then the compound **17** and **X3** were docked into the binding site of topoisomerase IIa as described for topoisomerase I. The grid site and dimensions are center_x: 26.529, center_y: 103.004, and center_z: 36.787 and size_x: 16, size_y: 16, and size_z: 16 respectively. For Vina docking, the default parameters were used if it was not mentioned [23, 24]. The best-scoring pose as judged by the Vina docking score was chosen and visually analyzed using PyMOL.

4.4. 3D-QSAR Modeling and Validation

Sybyl X 1.1 was used to perform the 3D-QSAR analyses. Two complementary methods were used: the Comparative Molecular Field Analysis (CoMFA) and the Comparative Molecular Similarity Indices Analysis (CoMSIA) [25]. For CoMFA field generation, we used the standard steric and electrostatic fields. The steric, electrostatic, hydrophobic, hydrogen bond donor and hydrogen bond acceptor fields were used for CoMSIA. Gasteiger-Hückel charges were assigned to all compounds. Other field settings were default. Partial least-squares (PLS) regression methods were used to derive models in this study. Leave-one-out (LOO) cross-validation was used to identify the optimum number of components. LOO approaches evaluate the predictability and over fitting of a regression model with the cross-validated correlation coefficient q^2. The non-cross-validated models were built with the optimum number of components over the entire training set and evaluated with the correlation coefficient (r^2), standard error of estimate (SEE), and F-test value. The resulting models were further validated using a test set of 10 compounds. The predictive r^2 (r^2_{pred}) indicates the correlation between the predicted and experimental activities of this test set.

Acknowledgments

This work was supported by a grant from the 973 Program (2010CB833802), NSFC Projects (81273384, 90913024).

REFERENCES

[1] J.C. Wang, DNA topoisomerases, Annu. Rev. Biochem. 65 (1996) 635-692.

[2] J.J. Champoux, DNA topoisomerases: structure, function, and mechanism, Annu. Rev. Biochem. 70 (2001) 369-413.

[3] C.C. Wu, T.K. Li, L. Farh, L.Y. Lin, T.S. Lin, Y.J. Yu, T.J. Yen, C.W. Chiang, N.L. Chan, Structural basis of type II topoisomerase inhibition by the anticancer drug etoposide, Science 333 (2011) 459-462.

[4] C.-L. Chen, F.-L. Liu, C.-C. Lee, T.-C. Chen, W.-W. Chang, J.-H. Guh, A.A. Ahmed Ali, D.-M. Chang, H.-S. Huang, Ring fusion strategy for the synthesis of anthra[2,3-d]oxazole-2-thione-5,10-dione homologues as DNA topoisomerase inhibitors and as antitumor agents, Eur. J. Med. Chem. 87 (2014) 30-38.

[5] P. Daumar, B.M. Zeglis, N. Ramos, V. Divilov, K.K. Sevak, N. Pillarsetty, J.S. Lewis, Synthesis and evaluation of 18F-labeled ATP competitive inhibitors of topoisomerase II as probes for imaging topoisomerase II expression, Eur. J. Med. Chem. 86 (2014) 769-781.

[6] K.-Y. Jun, H. Kwon, S.-E. Park, E. Lee, R. Karki, P. Thapa, J.-H. Lee, E.-S. Lee, Y. Kwon, Discovery of dihydroxylated 2,4-diphenyl-6-thiophen-2-yl-pyridine as a non-intercalative DNA-binding topoisomerase II-specific catalytic inhibitor, Eur. J. Med. Chem. 80 (2014) 428-438.

[7] T.M. Kadayat, C. Park, K.-Y. Jun, T.B. Thapa Magar, G. Bist, H.Y. Yoo, Y. Kwon, E.-S. Lee, Hydroxylated 2,4-diphenyl indenopyridine derivatives as a selective non-intercalative topoisomerase IIα catalytic inhibitor, Eur. J. Med. Chem. 90 (2015) 302-314.

[8] G.S. Basarab, J.I. Manchester, S. Bist, P.A. Boriack-Sjodin, B. Dangel, R. Illingworth, B.A. Sherer, S. Sriram, M. Uria-Nickelsen, A.E. Eakin, Fragment-to-hit-to-lead discovery of a novel pyridylurea scaffold of ATP competitive dual targeting type II topoisomerase inhibiting antibacterial agents, J. Med. Chem. 56 (2013) 8712-8735.

[9] T.A. Jarvinen, E.T. Liu, Topoisomerase IIalpha gene (TOP2A) amplification and deletion in cancer--more common than anticipated, Cytopathology 14 (2003) 309-313.

[10] A.M. Dingemans, H.M. Pinedo, G. Giaccone, Clinical resistance to topoisomerase-targeted drugs, Biochim. Biophys Acta. 1400 (1998) 275-288.

[11] K. Chikamori, A.G. Grozav, T. Kozuki, D. Grabowski, R. Ganapathi, M.K. Ganapathi, DNA topoisomerase II enzymes as molecular targets for cancer chemotherapy, Curr. Cancer Drug Targets 10 (2010) 758-771.

[12] J.P. Surivet, C. Zumbrunn, G. Rueedi, C. Hubschwerlen, D. Bur, T. Bruyere, H. Locher, D. Ritz, W. Keck, P. Seiler, C. Kohl, J.C. Gauvin, A. Mirre, V. Kaegi, M. Dos Santos, M. Gaertner, J. Delers, M. Enderlin-Paput, M. Boehme, Design, synthesis, and characterization of novel tetrahydropyran-based bacterial topoisomerase inhibitors with potent anti-gram-positive activity, J. Med. Chem. 56 (2013) 7396-7415.

[13] J. Qiu, B. Zhao, Y. Shen, W. Chen, Y. Ma, Y. Shen, A novel p-terphenyl derivative inducing cell-cycle arrest and apoptosis in MDA-MB-435 cells through topoisomerase inhibition, Eur. J. Med. Chem. 68 (2013) 192-202.

[14] R.D. Cramer, D.E. Patterson, J.D. Bunce, Comparative molecular field analysis (CoMFA). 1. Effect of shape on binding of steroids to carrier proteins, J. Am. Chem. Soc. 110 (1988) 5959-5967.

[15] G. Klebe, U. Abraham, T. Mietzner, Molecular similarity indices in a comparative analysis (CoMSIA) of drug molecules to correlate and predict their biological activity, J. Med. Chem. 37 (1994) 4130-4146.

[16] C. Da, S.L. Mooberry, J.T. Gupton, G.E. Kellogg, How to deal with low-resolution target structures: using SAR, ensemble docking, hydropathic analysis, and 3D-QSAR to definitively map the alphabeta-tubulin colchicine site, J. Med. Chem. 56 (2013) 7382-7395.

[17] M. Roberti, D. Pizzirani, M. Recanatini, D. Simoni, S. Grimaudo, A. Di Cristina, V. Abbadessa, N. Gebbia, M. Tolomeo, Identification of a terphenyl derivative that blocks the cell cycle in the G0-G1 phase and induces differentiation in leukemia cells, J. Med. Chem. 49 (2006) 3012-3018.

[18] J. Carmichael, W.G. DeGraff, A.F. Gazdar, J.D. Minna, J.B. Mitchell, Evaluation of a tetrazolium-based semiautomated colorimetric assay: assessment of chemosensitivity testing, Cancer Res. 47 (1987) 936-942.

[19] Y. Huang, J. Wang, G. Li, Z. Zheng, W. Su, Antitumor and antifungal activities in endophytic fungi isolated from pharmaceutical plants Taxus mairei, Cephalataxus fortunei and Torreya grandis, FEMS Immunol. Med. Microbiol. 31 (2001) 163-167.

[20] M. Fukuda, K. Nishio, F. Kanzawa, H. Ogasawara, T. Ishida, H. Arioka, K. Bojanowski, M. Oka, N. Saijo, Synergism between cisplatin and topoisomerase I inhibitors, NB-506 and SN-38, in human small cell lung cancer cells, Cancer Res. 56 (1996) 789-793.

[21] J.F. Barrett, J.A. Sutcliffe, T.D. Gootz, In vitro assays used to measure the activity of topoisomerases, Antimicrob. Agents Chemother. 34 (1990) 1-7.

[22] O. Trott, A.J. Olson, AutoDock Vina: improving the speed and accuracy of docking with a new scoring function, efficient optimization, and multithreading, J. Comput. Chem. 31 (2010) 455-461.

[23] O.M. Bautista-Aguilera, G. Esteban, I. Bolea, K. Nikolic, D. Agbaba, I. Moraleda, I. Iriepa, A. Samadi, E. Soriano, M. Unzeta, J. Marco-Contelles, Design, synthesis, pharmacological evaluation, QSAR analysis, molecular modeling and ADMET of novel donepezil-indolyl hybrids as multipotent cholinesterase/monoamine oxidase inhibitors for the potential treatment of Alzheimer's disease, Eur. J. Med. Chem. 75 (2014) 82-95.

[24] W. Zhan, D. Li, J. Che, L. Zhang, B. Yang, Y. Hu, T. Liu, X. Dong, Integrating docking scores, interaction profiles and molecular descriptors to improve the accuracy of molecular docking: Toward the discovery of novel Akt1 inhibitors, Eur. J. Med. Chem. 75 (2014) 11-20.

[25] J. Perez-Villanueva, J.L. Medina-Franco, T.R. Caulfield, A. Hernandez-Campos, F. Hernandez-Luis, L. Yepez-Mulia, R. Castillo, Comparative molecular field analysis (CoMFA) and comparative molecular similarity indices analysis (CoMSIA) of some benzimidazole derivatives with trichomonicidal activity, Eur. J. Med. Chem. 46 (2011) 3499-3508.

Figure 1. Compounds **1**-**20** and **X1-3.**

Figure 2. TOP1 (**A**) and TOP2α (B) inhibitory effects of compounds **2**, **12** and **17** in agarose relaxation assay. Negatively supercoiled pBR322 (SC) and relaxed DNA (RLX) are shown. 100 μM OPT (10-hydroxy camptothecin) and VP16 (etoposide) were employed as positive controls.

Figure 3. Compounds **17** and **X3** were docked into the TOP1 (A) and TOP2α (B)binding pockets. Compound **17** is shown in gray and compound **X3** is displayed in cyan. The docking results are illustrated by PyMoL [http://www.pymol.org/].

Figure 4. Structure of compounds **C1-5**

Figure 5. Scatter plots of predicted pIC_{50} values vs. experimental pIC_{50} values. The plots were obtained from the CoMFA (A) and CoMSIA (B) models. The training set contains 13 compounds (black squares), and the test set contains 10 compounds (red triangles).

Figure 6. Contour maps of the CoMFA (A) and CoMSIA (B) models with compound **17**. The green and yellow contours represent favorable and unfavorable steric substitutions, respectively, whereas the red and blue contours indicate a favorable effect from *more* electronegative and *more* electropositive substitutions, respectively.

Scheme 1-4. Synthesis route of compounds 1-20[a].

Table 1. Effect of compounds **1**-**20** on MDA-MB-435 cell proliferation[a]

Table 2. Summary of 3D-QSAR model statistics.

Table 3. Experimental pIC_{50} and predicted pIC_{50} values of the training set from the CoMFA and CoMSIA models.[a]

Table 4. Experimental pIC_{50} and predicted pIC_{50} values of the test set from the CoMFA and CoMSIA models.[a]

Table 1. The effect of compounds **1**-**20** on the proliferations of MDA-MB-435 cells[a]

Compound	IC_{50} (μM)	Compound	IC_{50} (μM)	Compound	IC_{50} (μM)
1	44.80±1.48	**8**	>100	**15**	>100
2	20.90±1.36	**9**	61.80±2.83	**16**	90.80±1.57
3	>100	**10**	41.80±1.39	**17**	3.96±1.07
4	>100	**11**	>100	**18**	>100
5	99.80±2.91	**12**	14.70±1.53	**19**	23.10±1.28
6	36.80±1.79	**13**	96.80±2.97	**20**	>100
7	>100	**14**	>100	**VP-16**	2.81±1.65

[a]The cytotoxicity of compounds was expressed as IC_{50}. The IC_{50} is defined as the concentration of compound that resulted in 50% inhibition of growth rate. Values represent means±SD of three individual experiments. VP-16 (etoposide) was used as positive compound.

Table 2. Summary of 3D-QSAR Model Statistics

Statistical parameters	CoMFA(IC_{50})	CoMSIA(IC_{50})
no. of components	4	5
$q2$ (cross-validated r^2)	0.605	0.622
r^2	0.998	0.994
std error of estimate	0.03	0.05
F value	960.9	242.5
r^2_{pred} (for test set)	0.74	0.66

[a]Cross-validated correlation coefficient from LOO.

[b]Non-cross-validated correlation coefficient.

[c]Correlation coefficient for test set predictions.

Table 3. Experimental pIC_{50} and predicted pIC_{50} values of the training set from the CoMFA and CoMSIA models.[a]

Training set	Experimental	CoMFA		CoMSIA	
		Predicted	Residual	Predicted	Residual
3	4	3.99	0.01	3.941	0.059
4	4	4.05	-0.05	4.089	-0.089
5	4.0009	4.018	-0.0171	4.018	-0.0171
6	4.4342	4.404	0.0302	4.387	0.0472
8	4	3.981	0.019	4.005	-0.005
11	4	3.985	0.015	4.032	-0.032
12	4.8327	4.866	-0.0333	4.871	-0.0383
13	4.0141	3.997	0.0171	3.99	0.0241
15	4	3.982	0.018	3.997	0.003
16	4.0419	4.062	-0.0201	4.057	-0.0151
17	5.4023	5.406	-0.0037	5.387	0.0153
X2	4.6876	4.696	-0.0084	4.646	0.0416
X1	5.3872	5.363	0.0242	5.401	-0.0138

[a] $pIC_{50} = -\log(IC_{50})$, if the $IC_{50} > 100$, we determined the $pIC_{50} = 4$.

[b] The IC_{50} values of compound X1 and X2 were 0.39 ± 0.03 and 32.67 ± 6.03.

Table 4. Experimental pIC_{50} and predicted pIC_{50} values of the training set from the CoMFA and CoMSIA models.[a]

Training set	Experimental	CoMFA		CoMSIA	
		Predicted	Residual	Predicted	Residual
C1	4.4516	4.502	-0.0504	4.211	0.2406
C2	4.9974	4.809	0.1884	4.603	0.3944
C3	4.8901	4.786	0.1041	4.749	0.1411
C4	4.6461	4.713	-0.0669	4.361	0.2851
C5	4.9393	4.757	0.1823	4.404	0.5353
1	4.3487	4.302	0.0467	4.226	0.1227
2	4.6799	4.615	0.0649	4.452	0.2279
7	4	4.44	-0.44	4.187	-0.187
9	4.209	4.515	-0.306	4.292	-0.083
10	4.3788	4.476	-0.0972	4.295	0.0838

[a] $pIC_{50} = -\log (IC_{50})$, if the $IC_{50} > 100$, we determined the $pIC_{50} = 4$.

[b] The IC_{50} values of compounds C1-C5 were 35.35 ± 2.16, 10.06 ± 0.84, 12.88 ± 1.47, 22. 59 ± 1.59 and 11.50 ± 1.11.

Figure 1.

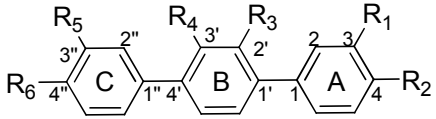

[1,1':4',1"-Terphenyl]-2',3,3',4,4"-pentaol (X1):
$R_1 = R_2 = R_3 = R_4 = R_6 = OH$, $R_5 = H$
[1,1':4',1"-Terphenyl]- 4"-monol,2',3,3',4-tetmethoxy (X2):
$R_1 = R_2 = R_3 = R_4 = OCH_3$, $R_5 = H$, $R_6 = OH$
[1,1':4',1"-Terphenyl]-3,4,4"-triol (X3):
$R_1 = R_2 = R_6 = OH$, $R_3 = R_4 = R_5 = H$
1: $R_1 = COOCH_3$, $R_2 = R_6 = OH$, $R_3 = R_4 = OCH_3$, $R_5 = H$
2: $R_1 = R_6 = OH$, $R_2 = COOCH_3$, $R_3 = R_4 = OCH_3$, $R_5 = H$,
3: $R_1 = COOH$, $R_2 = R_6 = OH$, $R_3 = R_4 = OCH_3$, $R_5 = H$
4: $R_1 = R_6 = OH$, $R_2 = COOH$, $R_3 = R_4 = OCH_3$, $R_5 = H$
5: $R_1 = COOH$, $R_2 = R_3 = R_4 = R_6 = OH$, $R_5 = H$
6: $R_1 = R_3 = R_4 = R_6 = OH$, $R_2 = COOH$, $R_5 = H$
7: $R_1 = R_2 = R_3 = R_4 = OCH_3$, $R_5 = H$, $R_6 = COOH$
8: $R_1 = R_2 = R_3 = R_4 = OH$, $R_5 = H$, $R_6 = COOH$
9: $R_1 = R_5 = NO_2$, $R_2 = R_6 = OH$, $R_3 = R_4 = OCH_3$
10: $R_1 = R_5 = H$, $R_2 = R_6 = OH$, $R_3 = R_4 = OC_2H_5$
11: $R_1 = R_2 = R_5 = R_6 = OCH3$, $R_3 = R_4 = OC_2H_5$
12: $R_1 = R_5 = H$, $R_2 = R_6 = OH$, $R_3 = R_4 = OCH_3$
13: $R_1 = R_5 = H$, $R_2 = R_6 = OCH_3$, $R_3 = R_4 = OCOCH_3$
14: $R_1 = R_2 = R_5 = R_6 = OCH3$, $R_3 = R_4 = OCOCH_3$
15: $R_1 = R_5 = H$, $R_2 = R_3 = R_4 = R_6 = OH$
16: $R_1 = R_2 = R_3 = R_4 = R_5 = R_6 = OCH_3$
17: $R_1 = R_2 = R_3 = R_4 = R_5 = R_6 = OH$

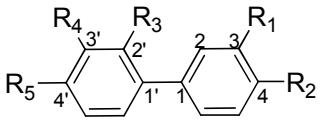

18: $R_1 = R_3 = R_4 = H$, $R_2 = R_5 = COOCH_3$
19: $R_1 = R_2 = R_3 = R_4 = OCH_3$, $R_5 = H$
20: $R_1 = R_4 = NO_2$, $R_2 = R_5 = OH$, $R_3 = H$

Figure 2.

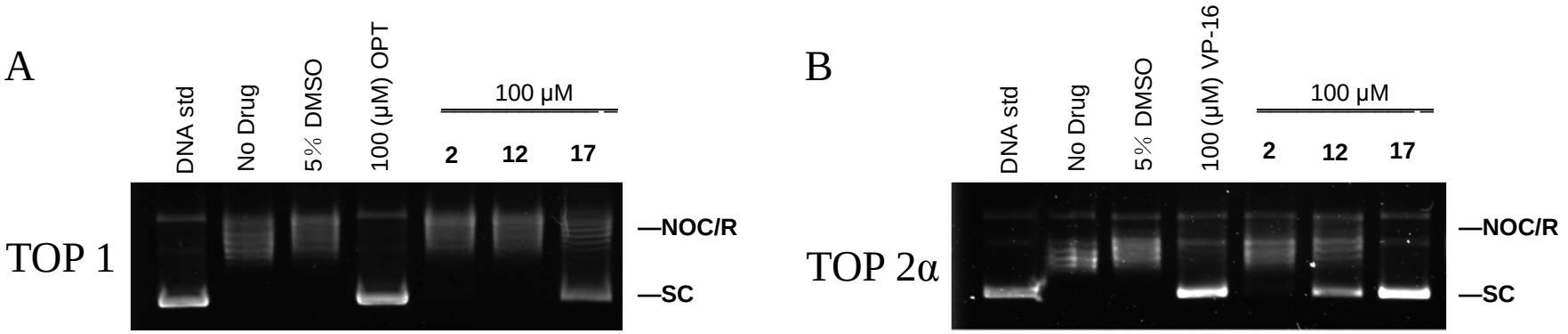

Figure 3.

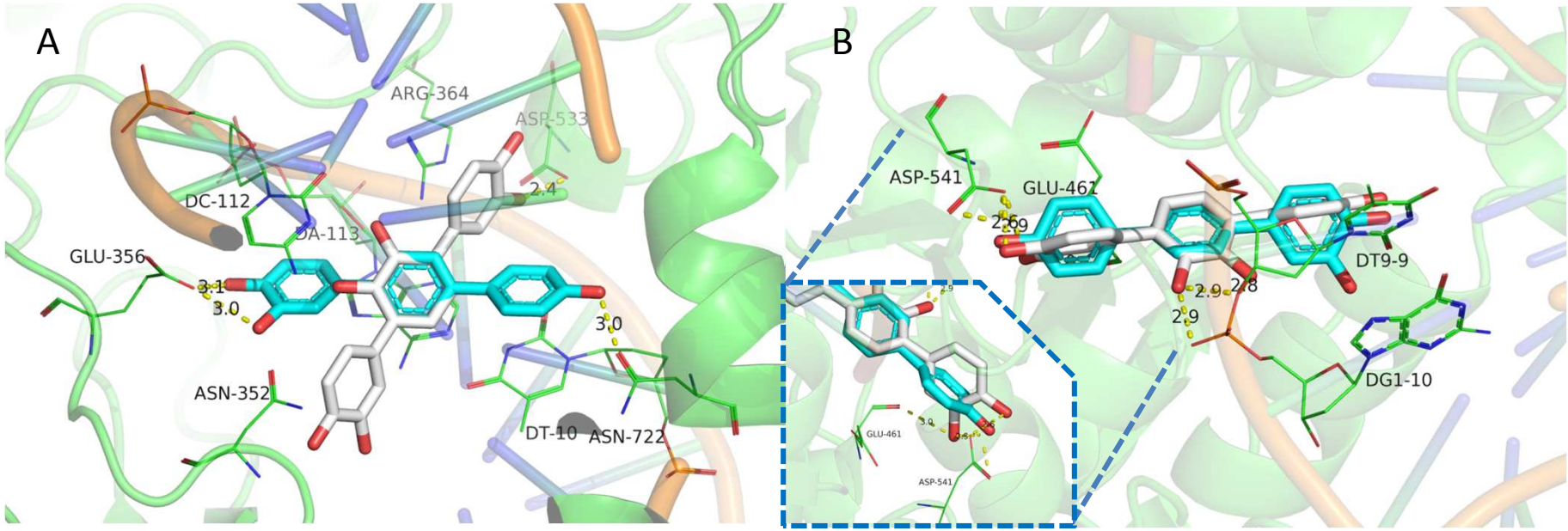
A
ARG-364
ASP-533
2.4
DC-112
DA-113
GLU-356
3.1
3.0
3.0
ASN-352
DT-10
ASN-722
B
ASP-541
GLU-461
2.69
DT9-9
2.9
2.8
2.9
DG1-10
GLU-461
ASP-541

Figure 4.

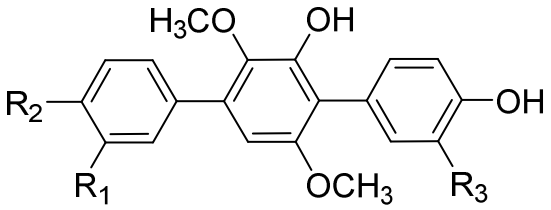

C1 $R_1 = R_3 = H$; $R_2 = OH$
C2 $R_1 = H$; $R_2 = R_3 = OH$
C3 $R_1 = R_2 = R_3 = OH$

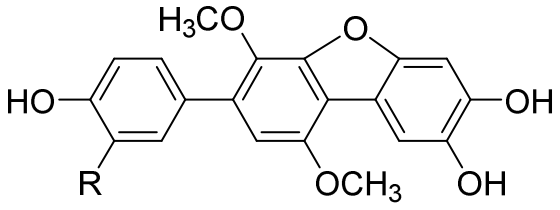

C4 R = H
C5 R = OH

Figure 5.

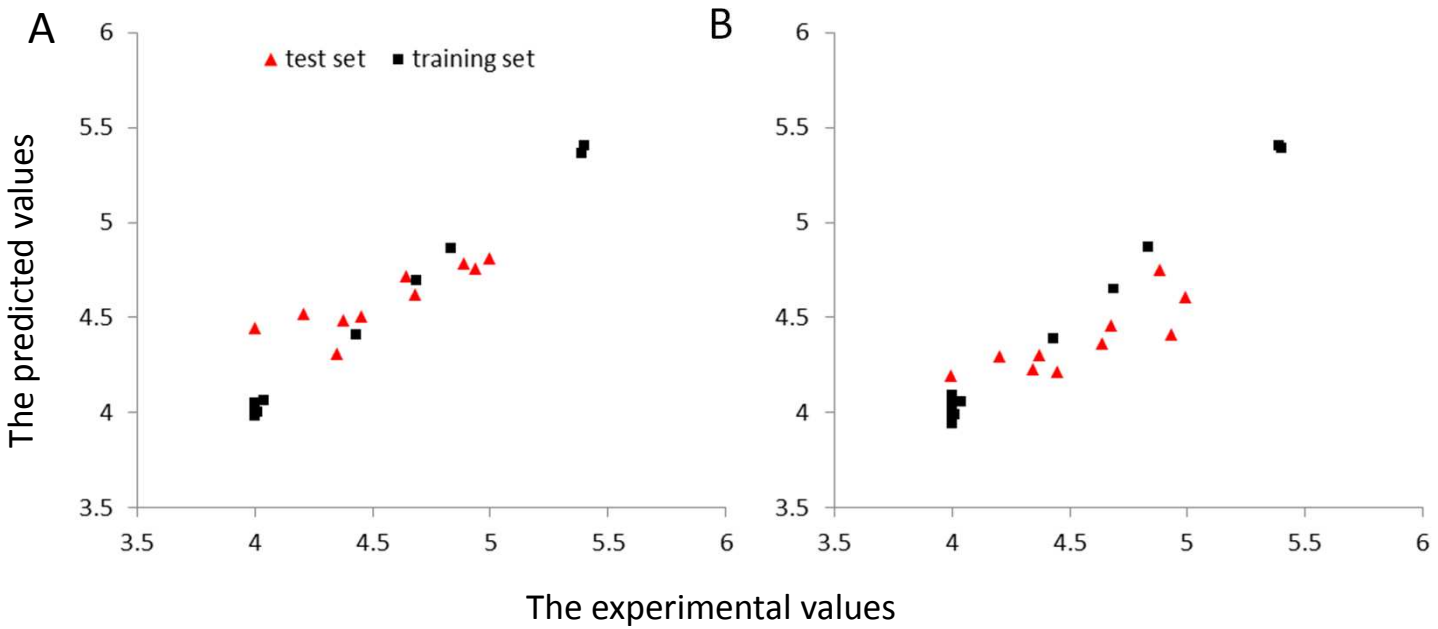
A
B
test set
training set
The predicted values
The experimental values
6
5.5
5
4.5
4
3.5
3.5
4
4.5
5
5.5
6

Figure 6.

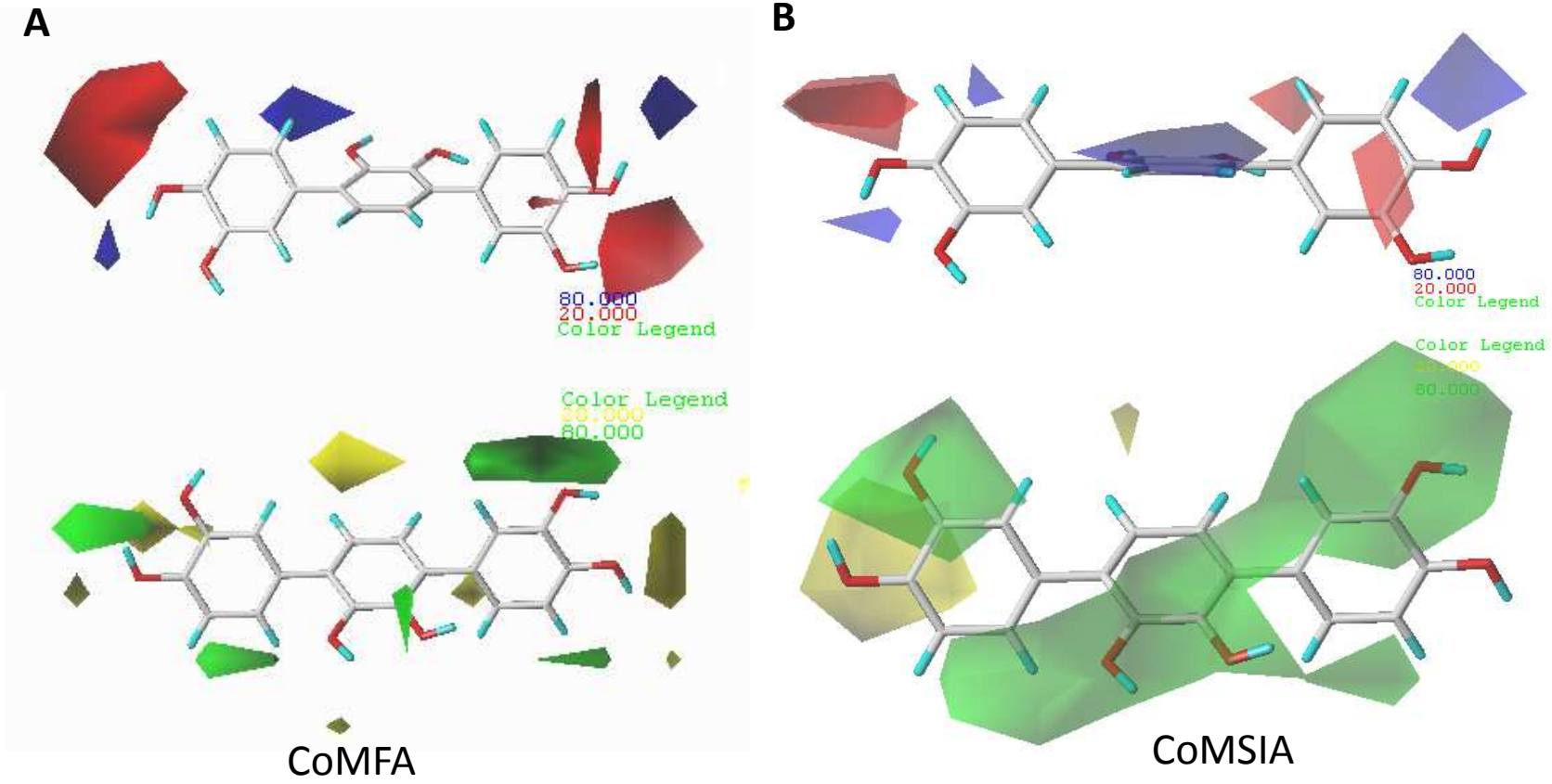
A
80.000
20.000
Color Legend
Color Legend
20.000
80.000
B
80.000
20.000
Color Legend
Color Legend
80.000
CoMFA
CoMSIA

Scheme 1-4.

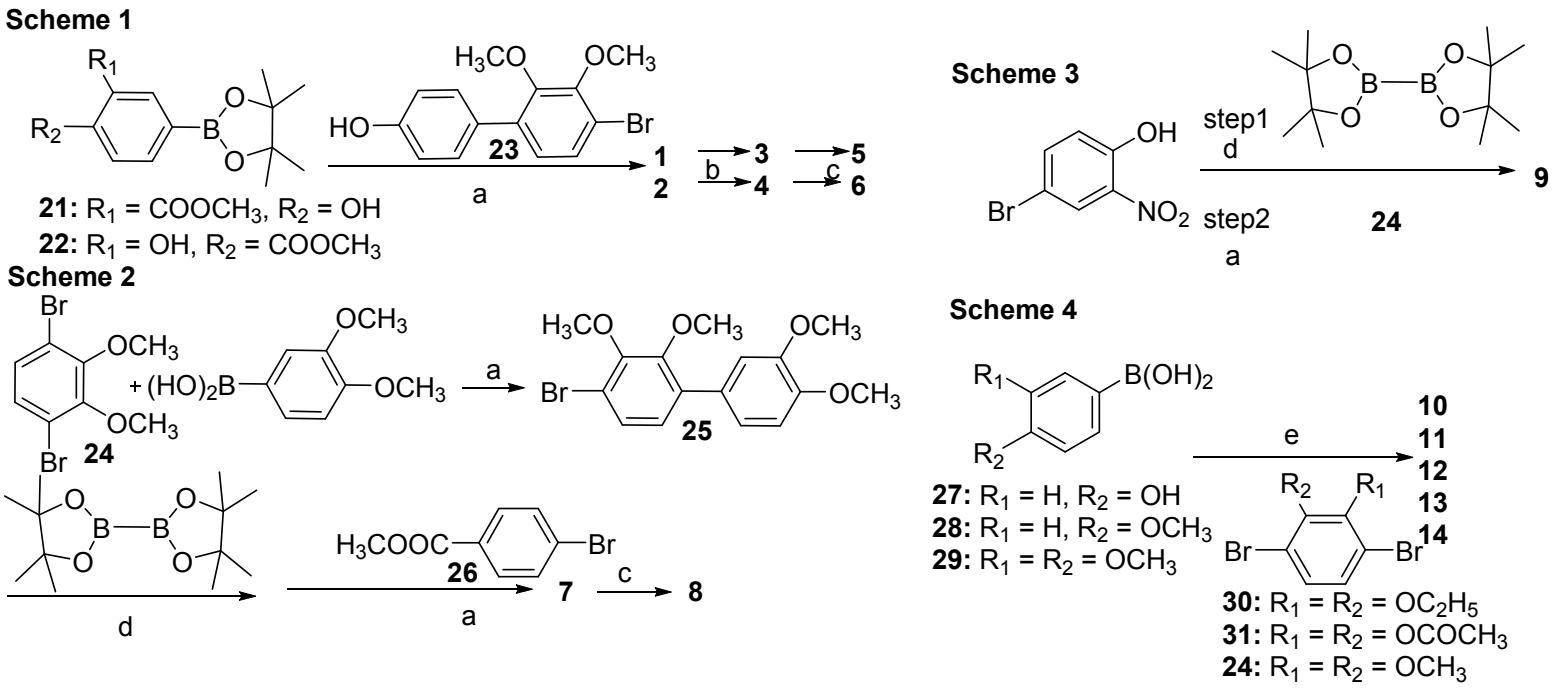

[a]Reagents and conditions: (a) Pd-DPPF, $KF{\cdot}2H_2O$; (b) KOH, 50% MeOH; (c) -20° C, BBr_3; (d) Pd-DPPF, KAc; (e) Pd-DPPF, $KF{\cdot}2H_2O$.

Highlights

- Synthesis and evaluation of a series of novel terphenyls inhibited TOP.
- The results of 3D-QSAR analysis were consistent with Docking analysis.
- The contour maps provide useful insight into designing novel TOP inhibitory.

CONTENTS

^{1}H NMR (600 MHz, $(CD_3)_2CO$, rt) of **1**

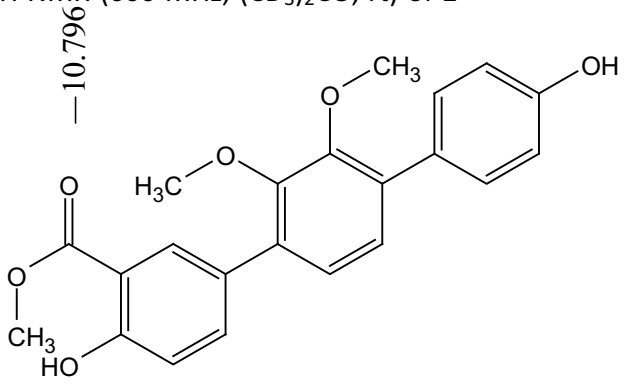

1

^{13}C NMR (150 MHz, $(CD_3)_2CO$, rt) of **1**

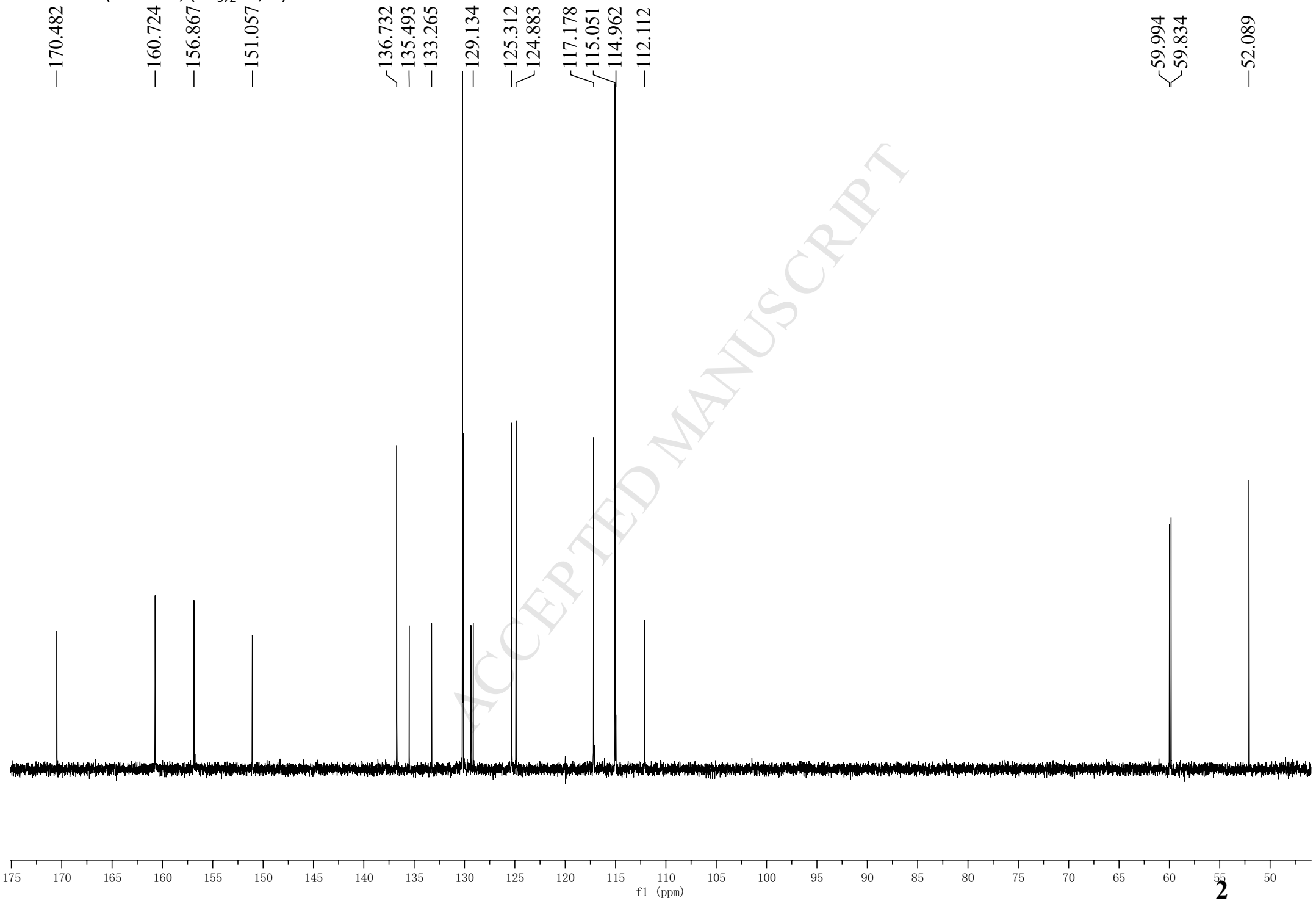

^{1}H NMR (600 MHz, $(CD_3)_2CO$, rt) of **2**

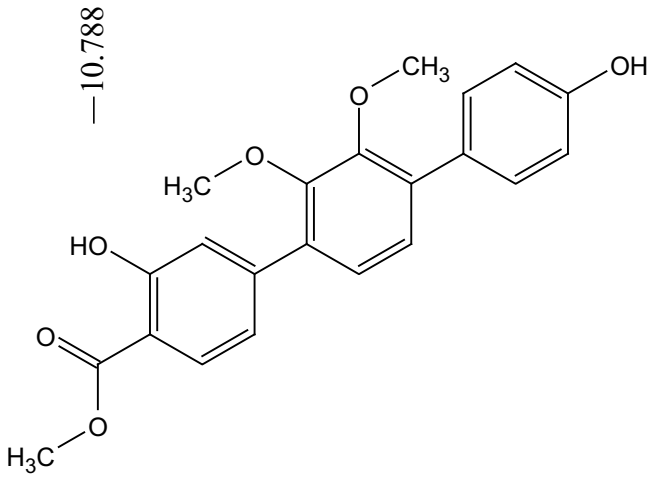

3

^{13}C NMR (150 MHz, $(CD_3)_2CO$, rt) of **2**

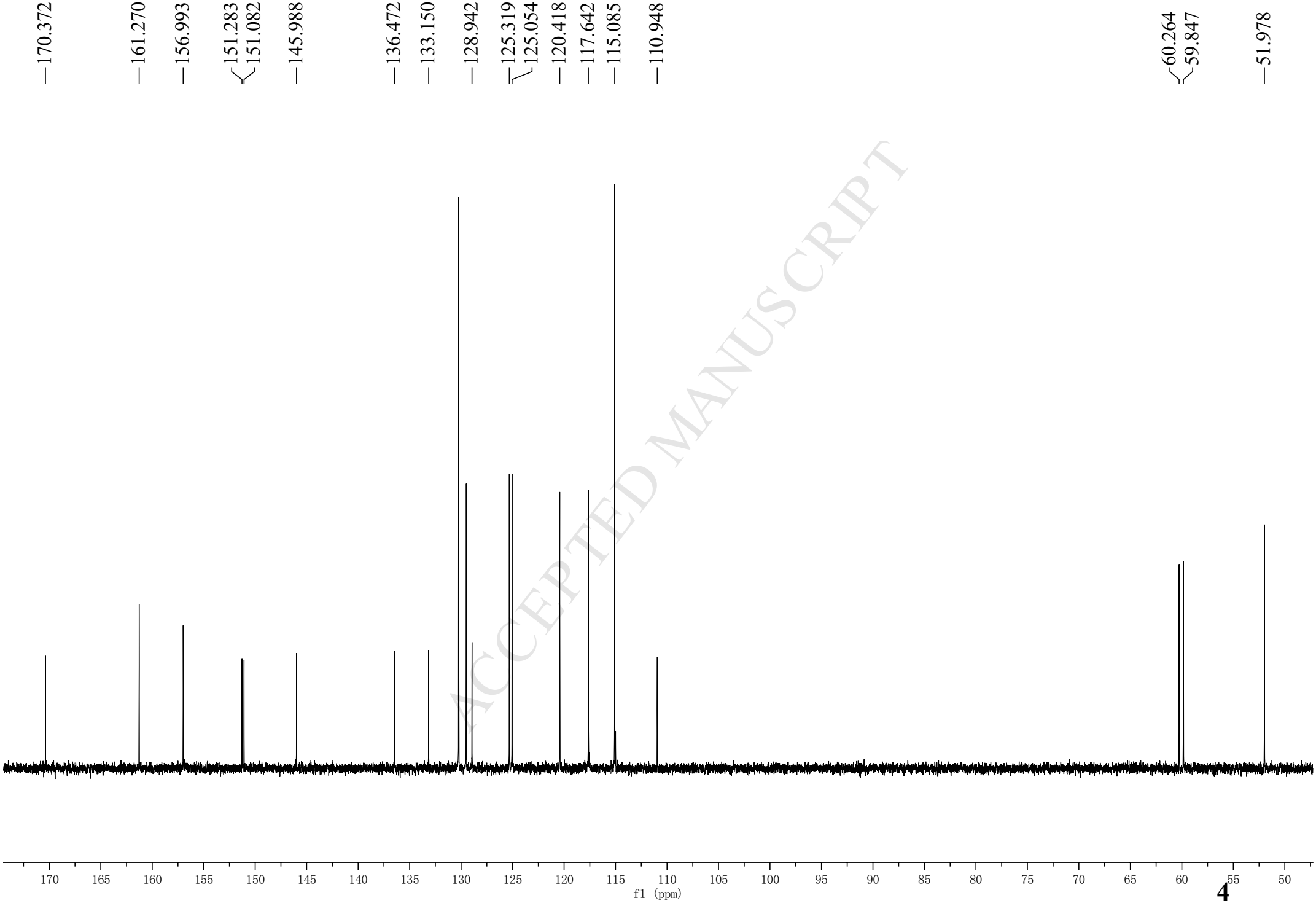

^{1}H NMR (600 MHz, $CO(CD_3)_2$ of **3**

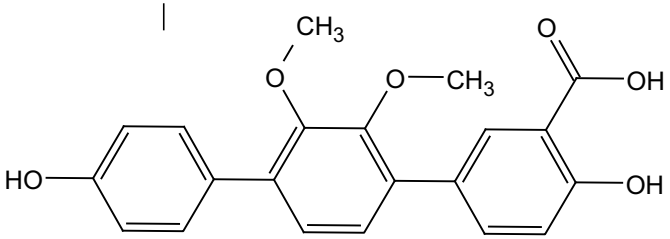

^{13}C NMR (150 MHz, $CO(CD_3)_2$ of **3**

171.835
161.338
156.843
151.067
136.802
135.434
133.326
129.125
125.330
124.922
117.073
115.033
112.019
60.008
59.837

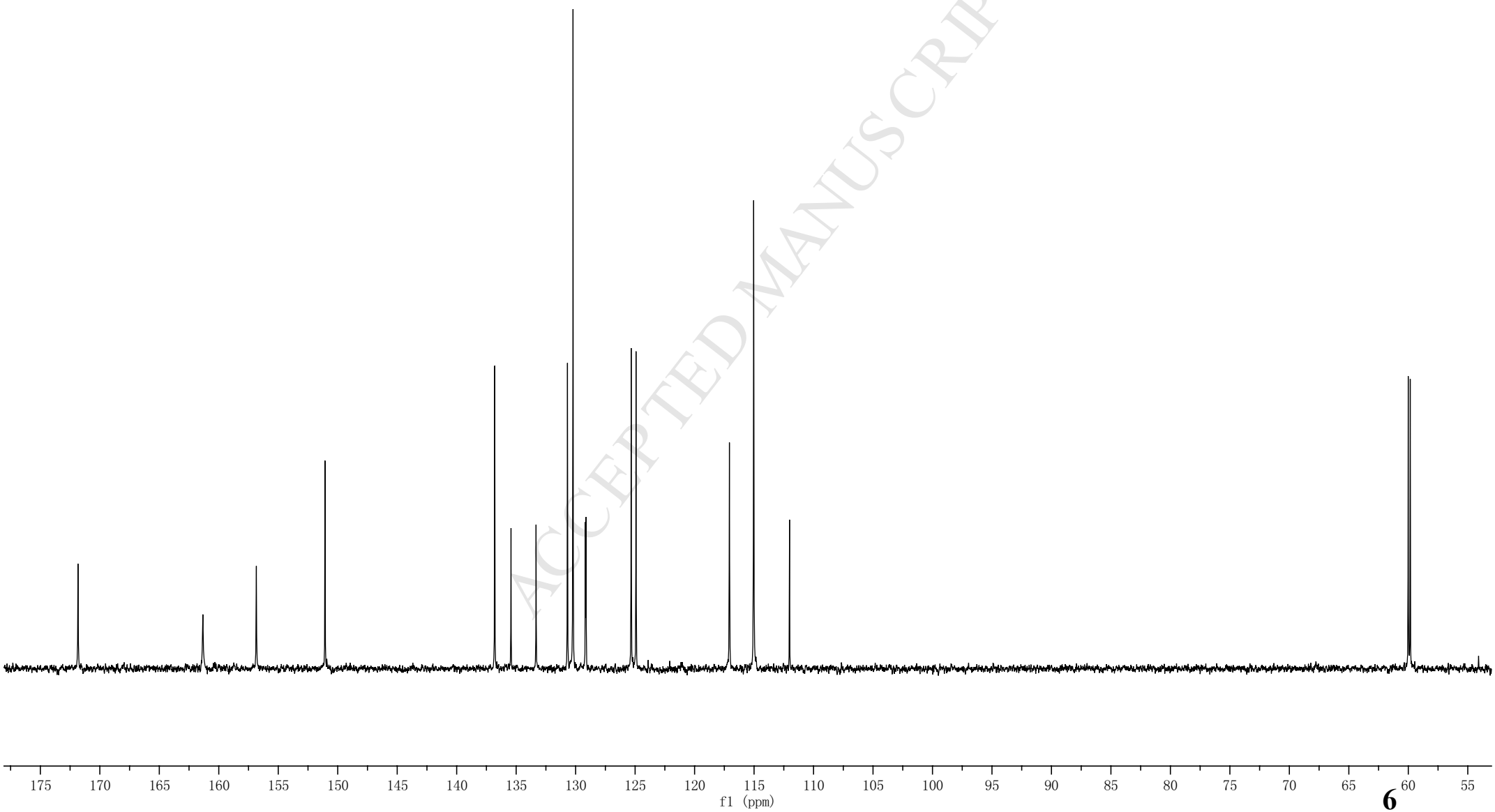

^{1}H NMR (600 MHz, $CO(CD_3)_2$ of **4**

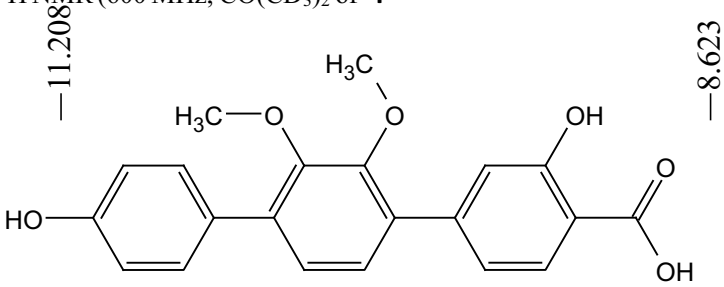

^{13}C NMR (150 MHz, $CO(CD_3)_2$ of **4**

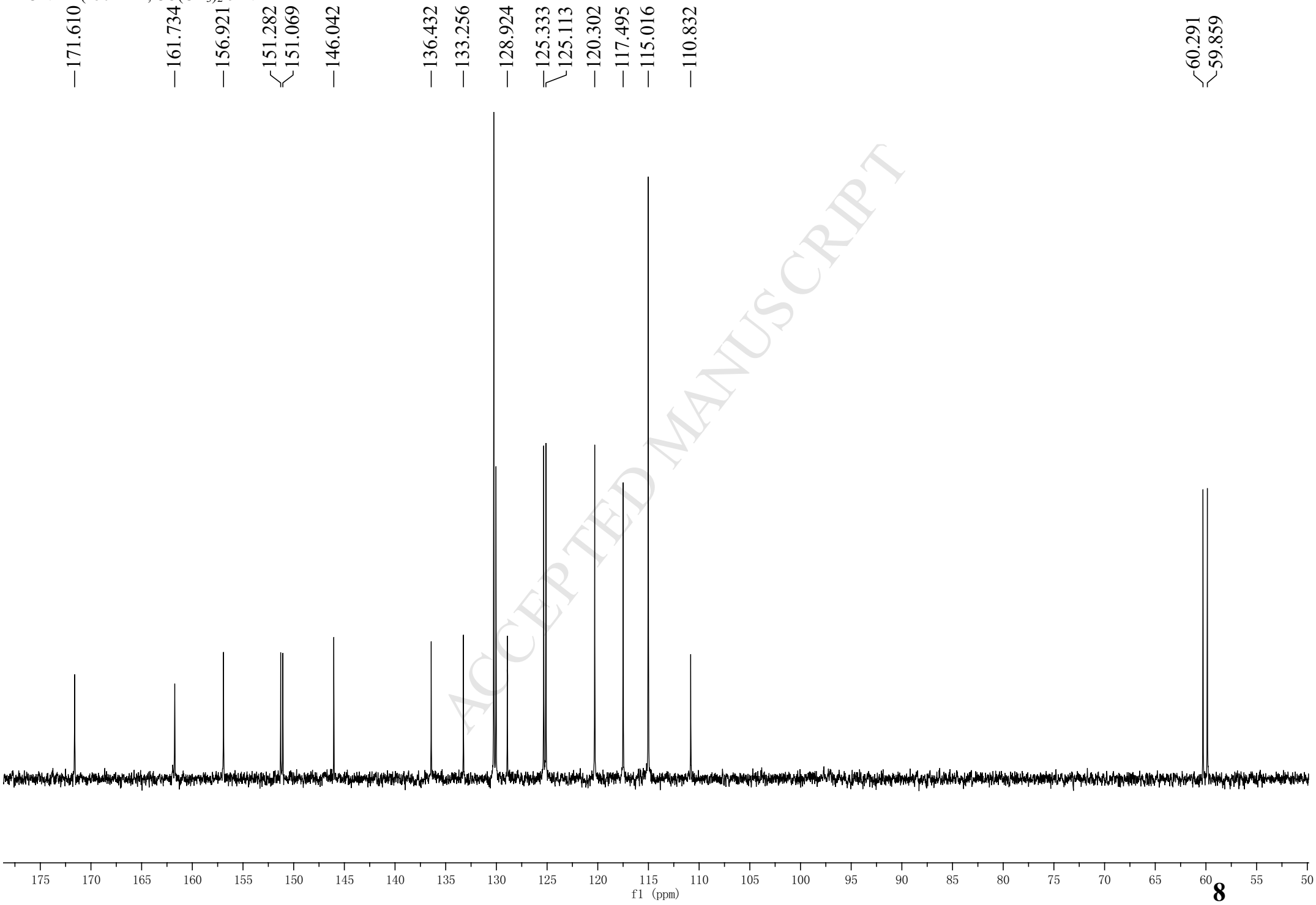

^{1}H NMR (600 MHz, $(CD_3)_2CO$, rt) of **5**

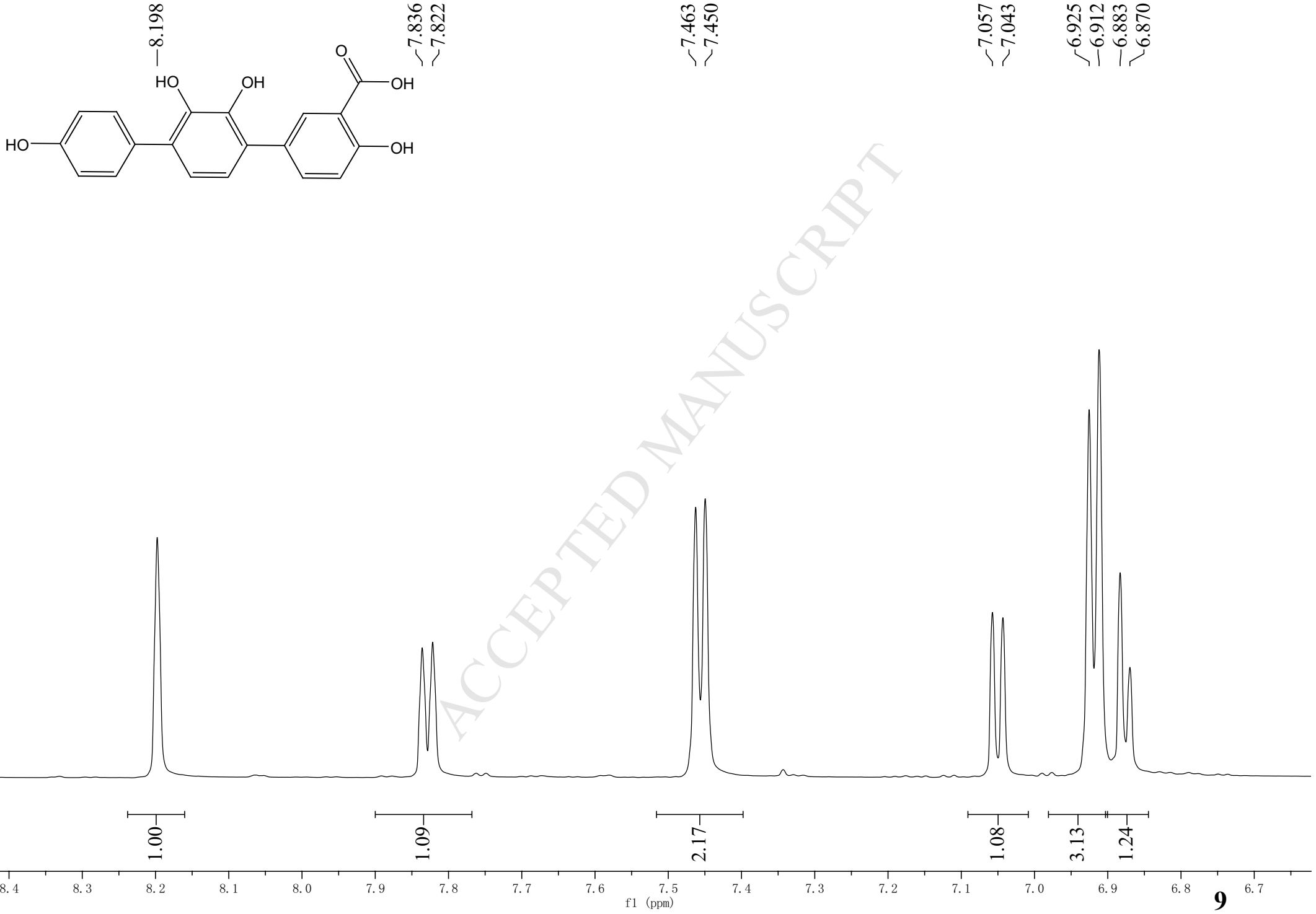

^{13}C NMR (150 MHz, $(CD_3)_2CO$, rt) of **5**

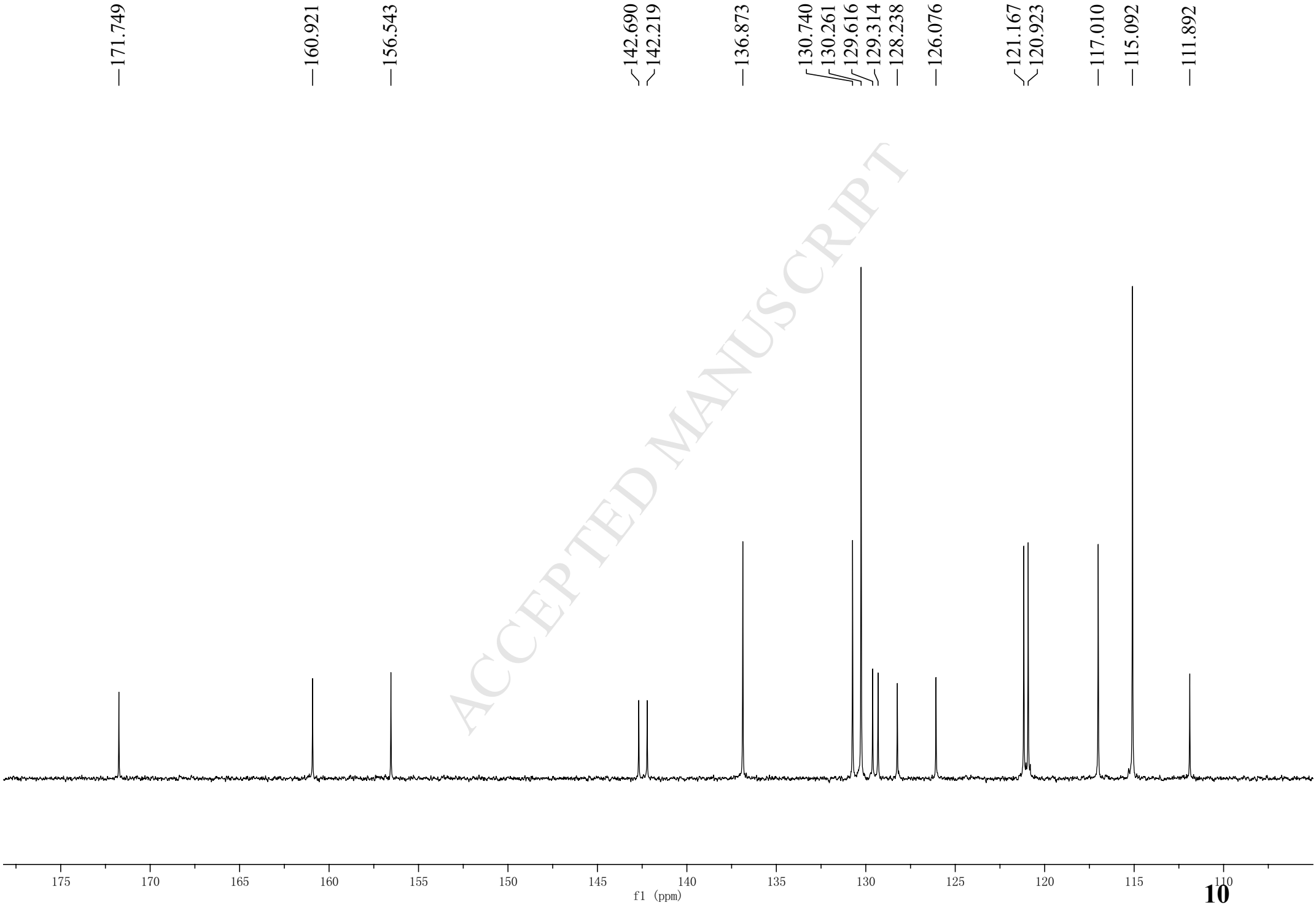

^{1}H NMR (600 MHz, $(CD_3)_2CO$, rt) of **6**

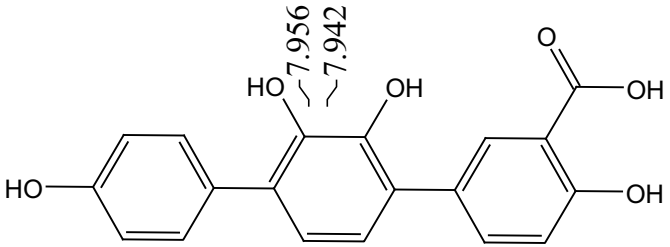

^{13}C NMR (150 MHz, $(CD_3)_2CO$, rt) of **6**

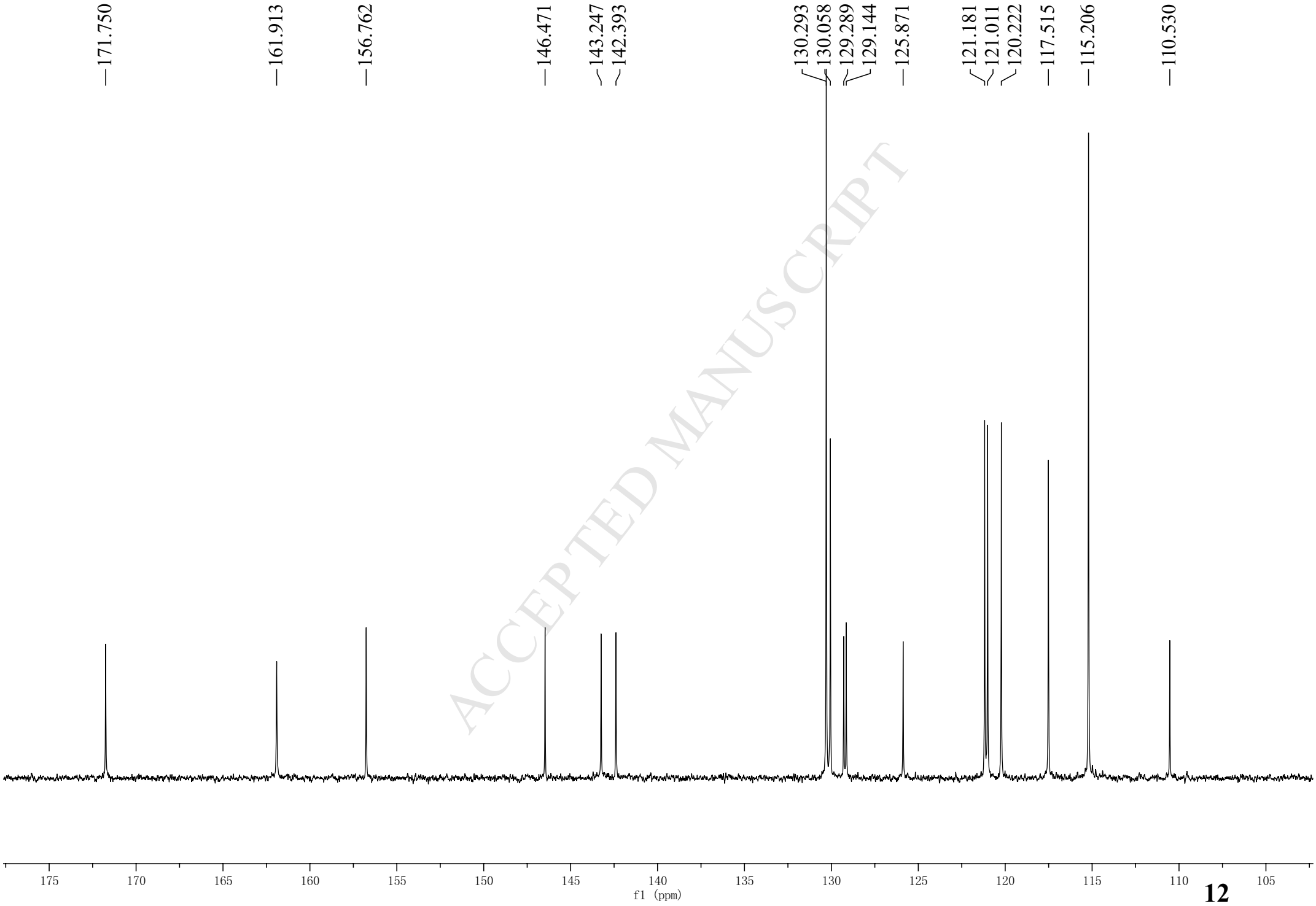

^{1}H NMR (600 MHz, DMSO-*d6*, rt) of **7**

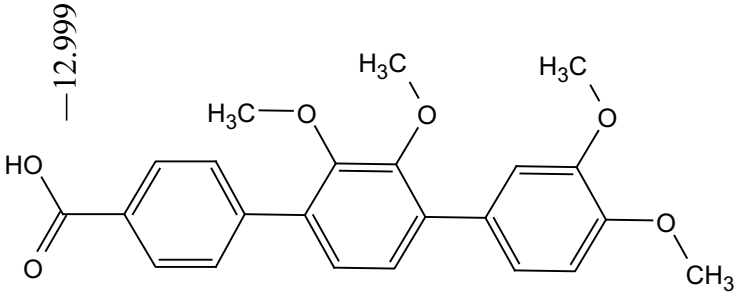

^{13}C NMR (150 MHz, DMSO-*d6*, rt) of **7**

167.65
151.19
151.05
148.80
148.75
142.46
135.98
133.88
129.55
125.67
121.63
113.07
112.06
61.13
60.86
55.96

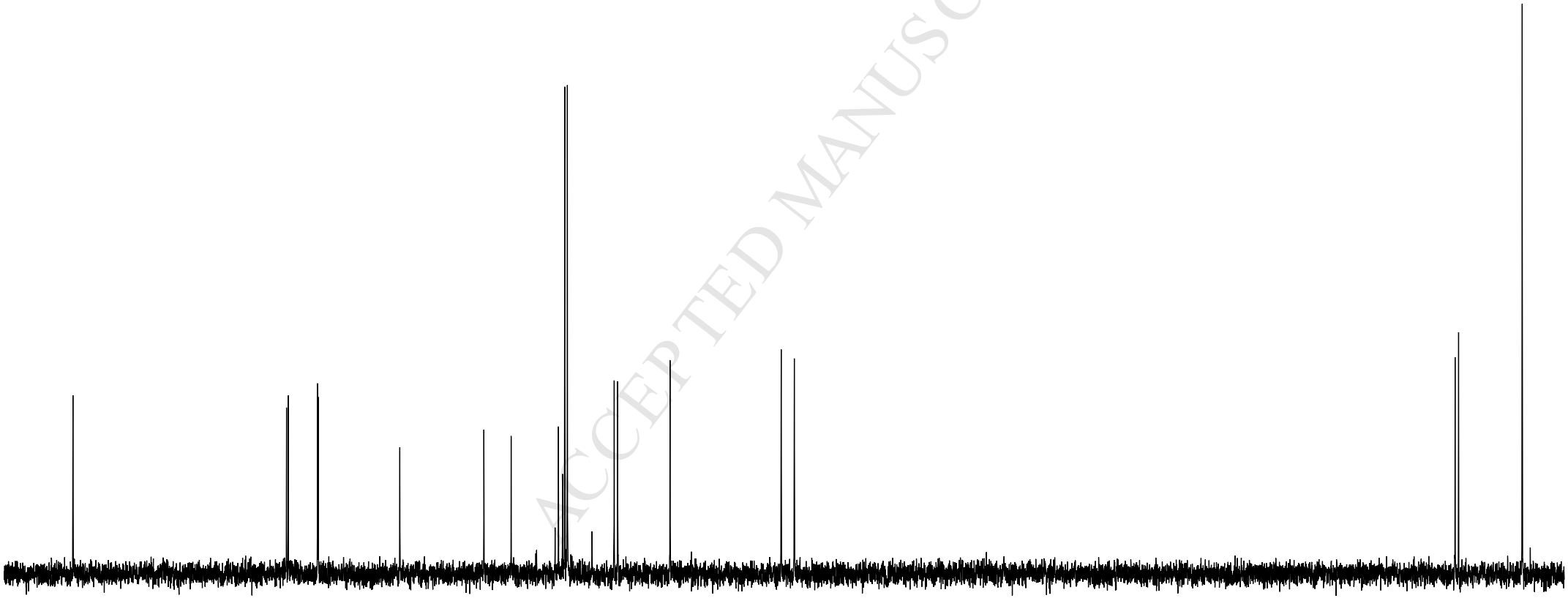

170 165 160 155 150 145 140 135 130 125 120 115 110 105 100 95 90 85 80 75 70 65 60 55

f1 (ppm)

^{1}H NMR (600 MHz, Methanol-d_4) of **8**

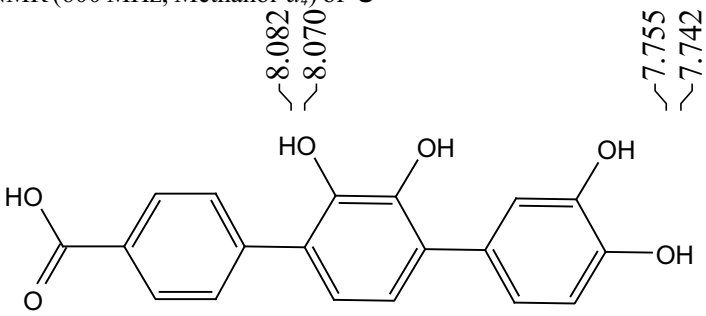

^{13}C NMR (150 MHz, Methanol-d_4) of **8**

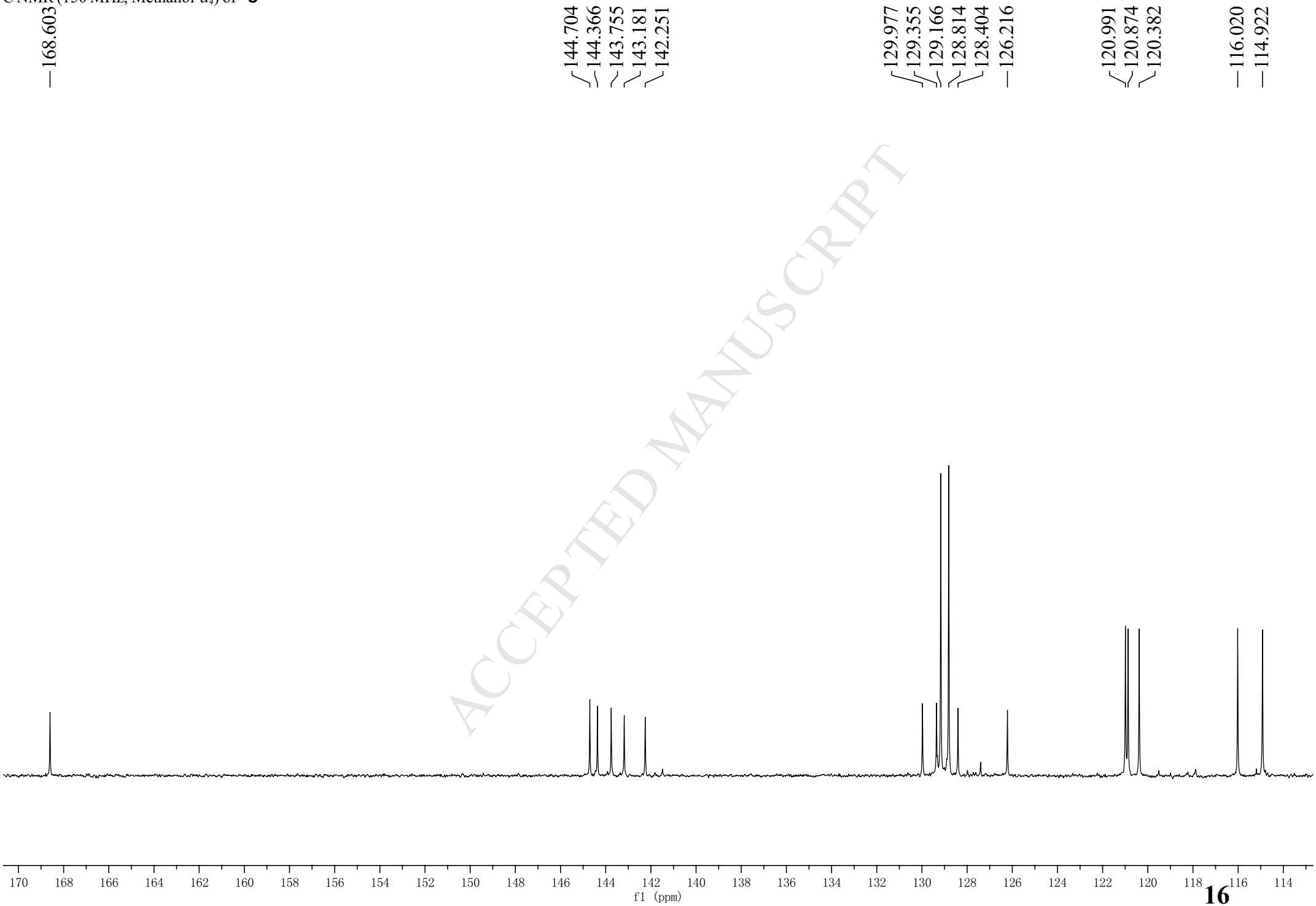

^{1}H NMR (600 MHz, $CDCl_3$, rt) of **9**

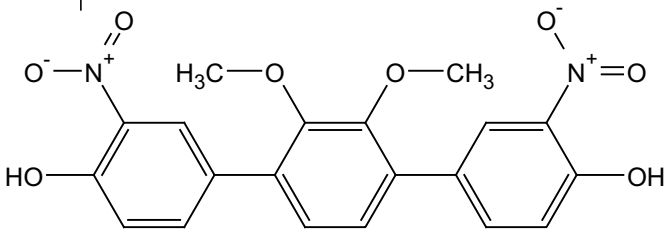

^{13}C NMR (150 MHz, $CDCl_3$, rt) of **9**

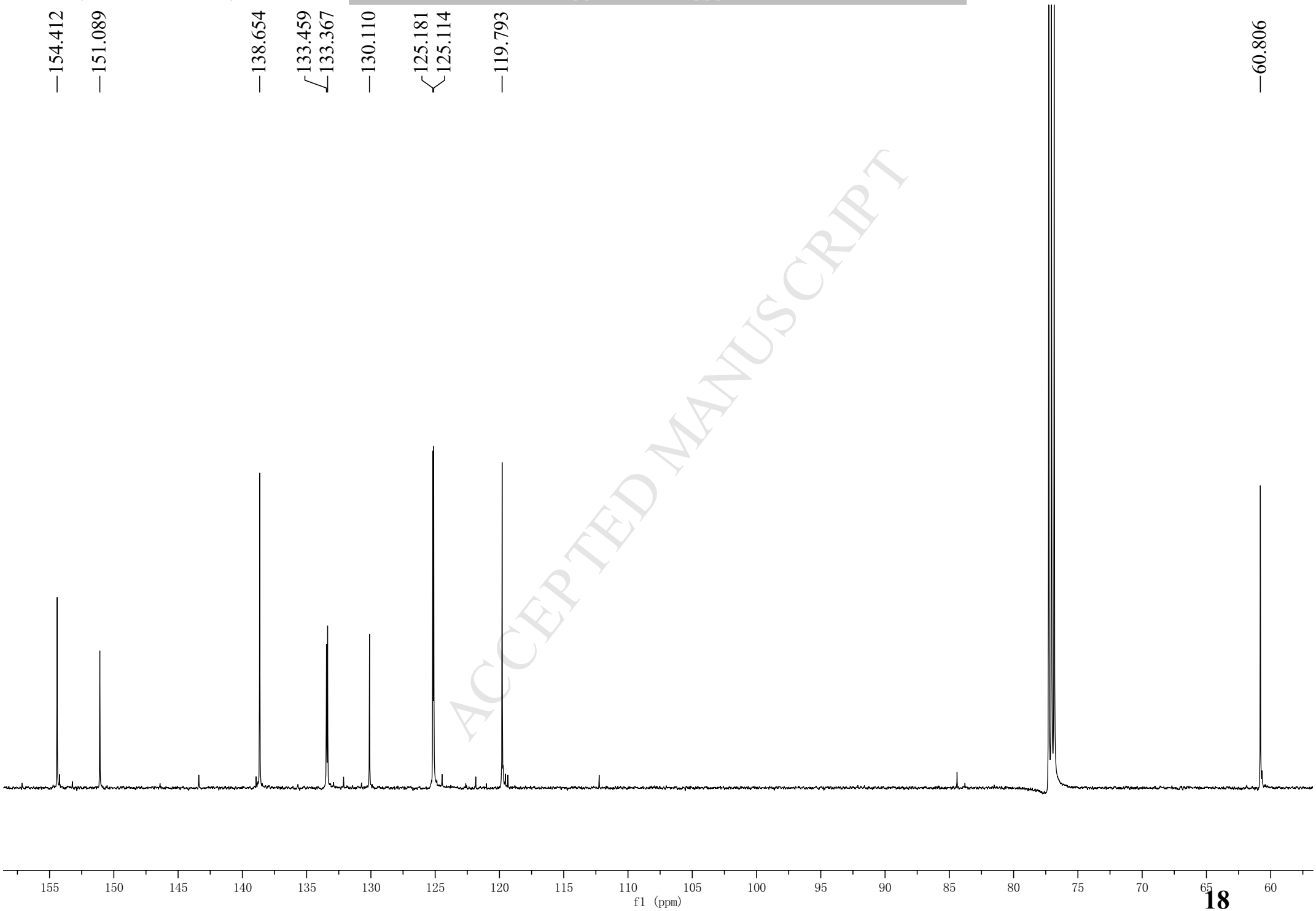

^{1}H NMR (600 MHz, CD_3OD, rt) of **10**

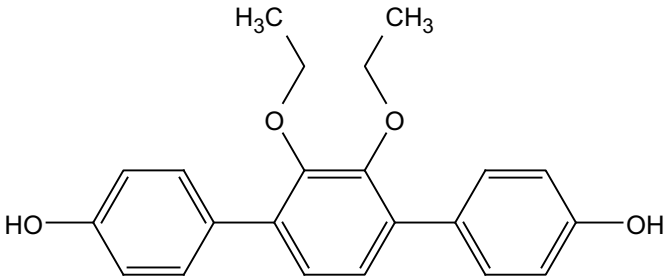

^{13}C NMR (150 MHz, CD_3OD, rt) of **10**

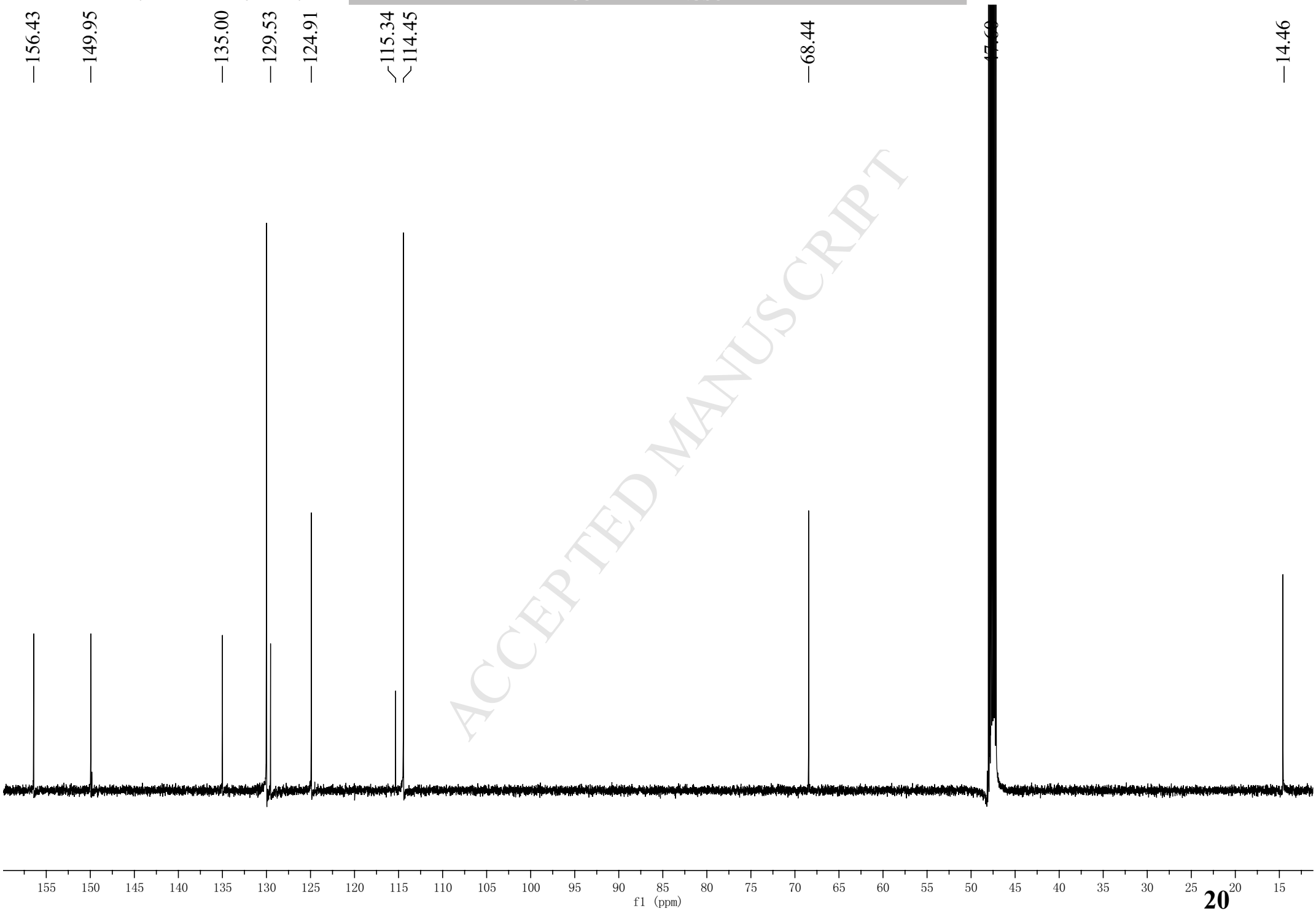

^{1}H NMR (600 MHz, $CDCl_3$, rt) of **11**

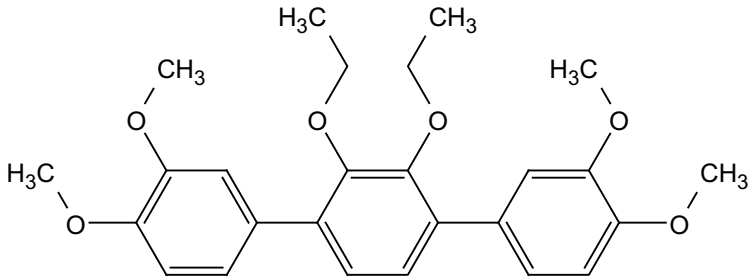

^{13}C NMR (150 MHz, $CDCl_3$, rt) of **11**

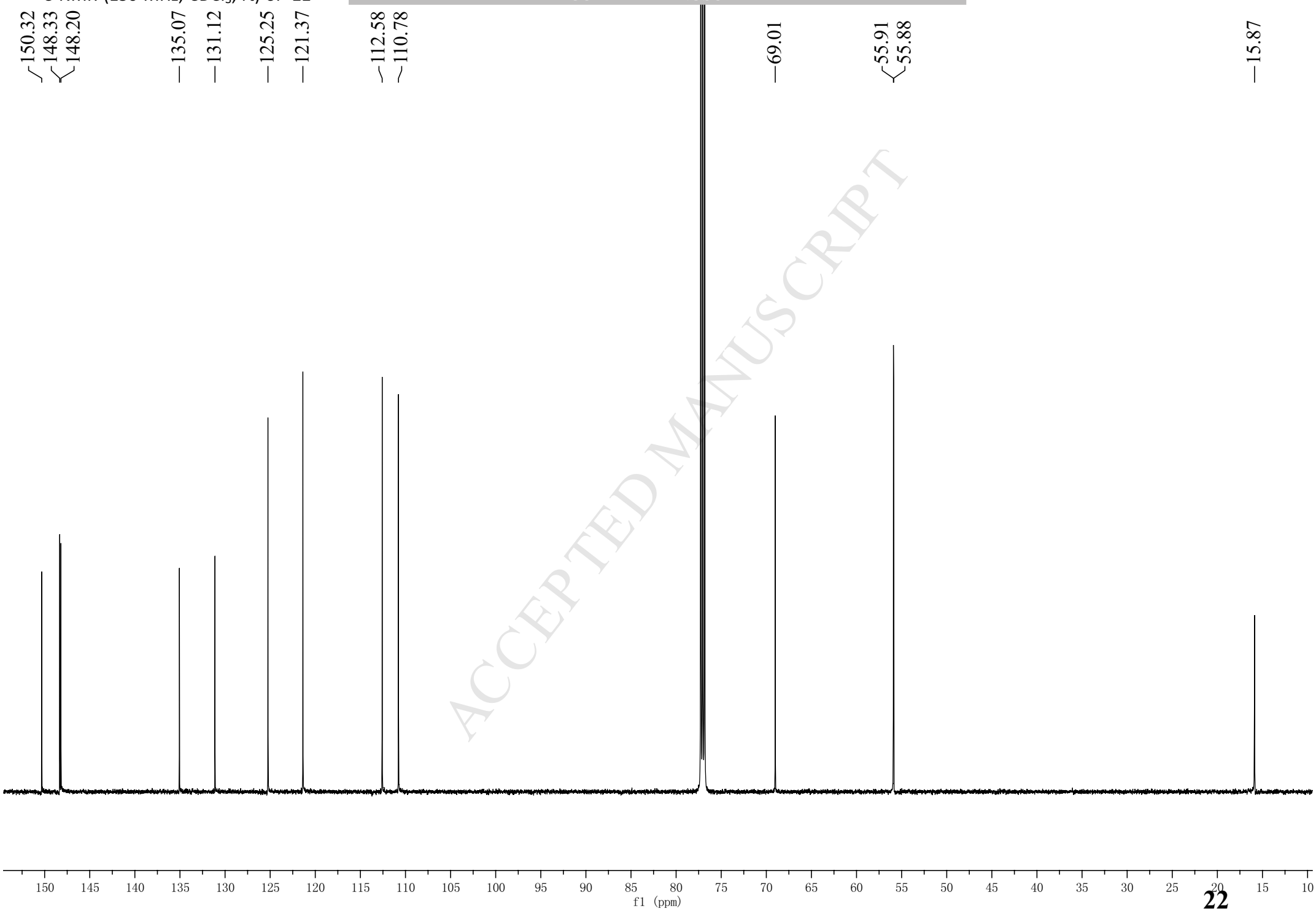

^{1}H NMR (600 MHz, CD_3OD, rt) of **12**

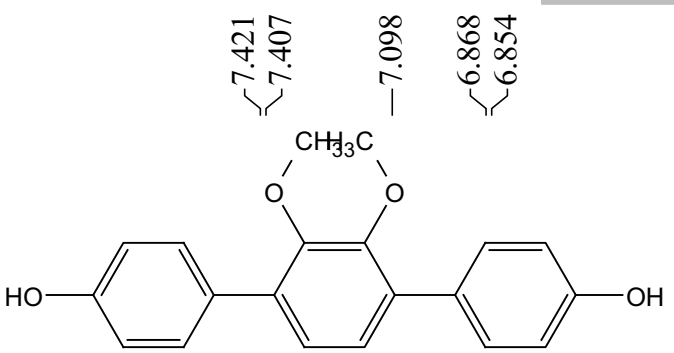

^{13}C NMR (150 MHz, CD_3OD, rt) of **12**

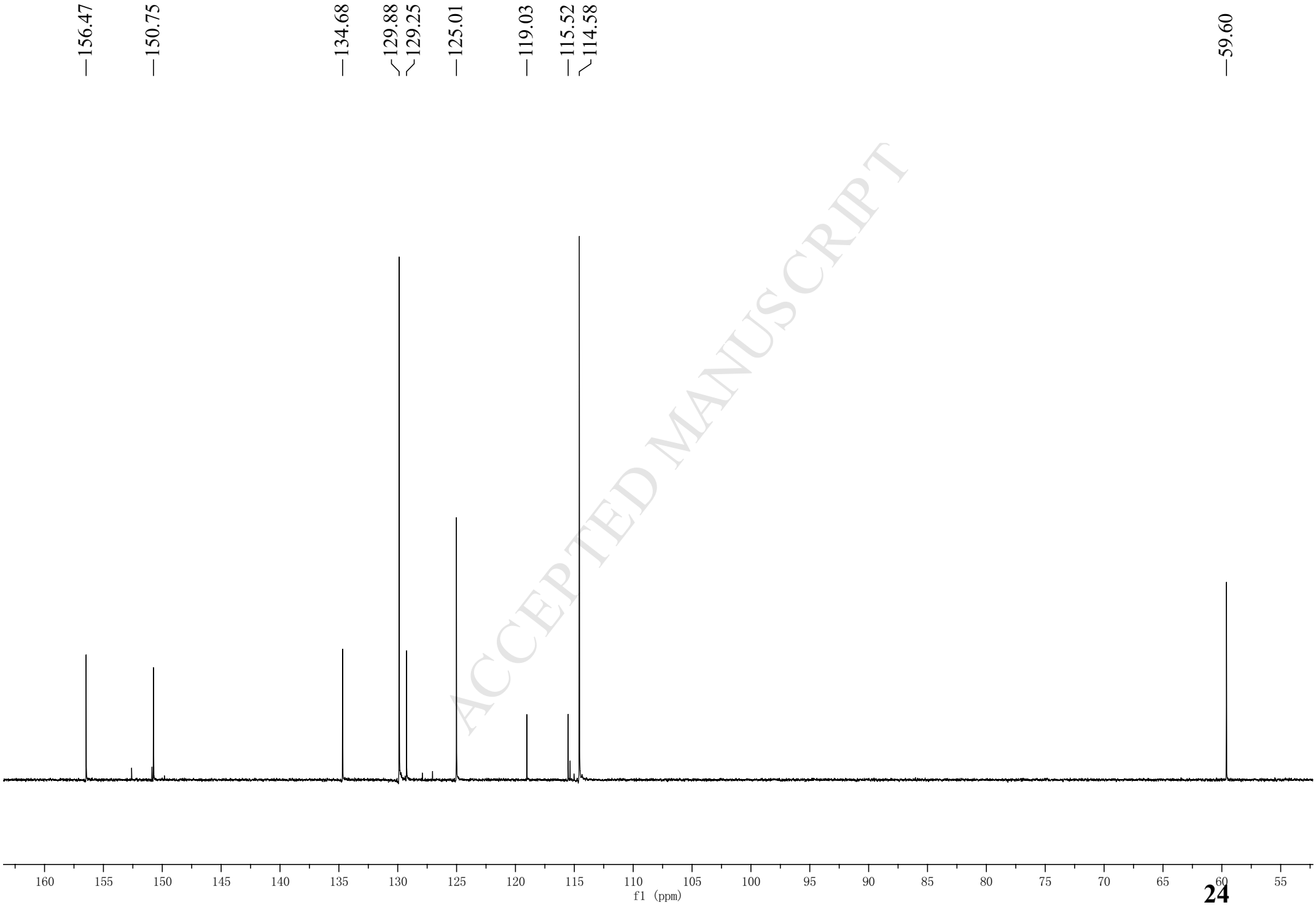

^{1}H NMR (600 MHz, $CDCl_3$, rt) of **13**

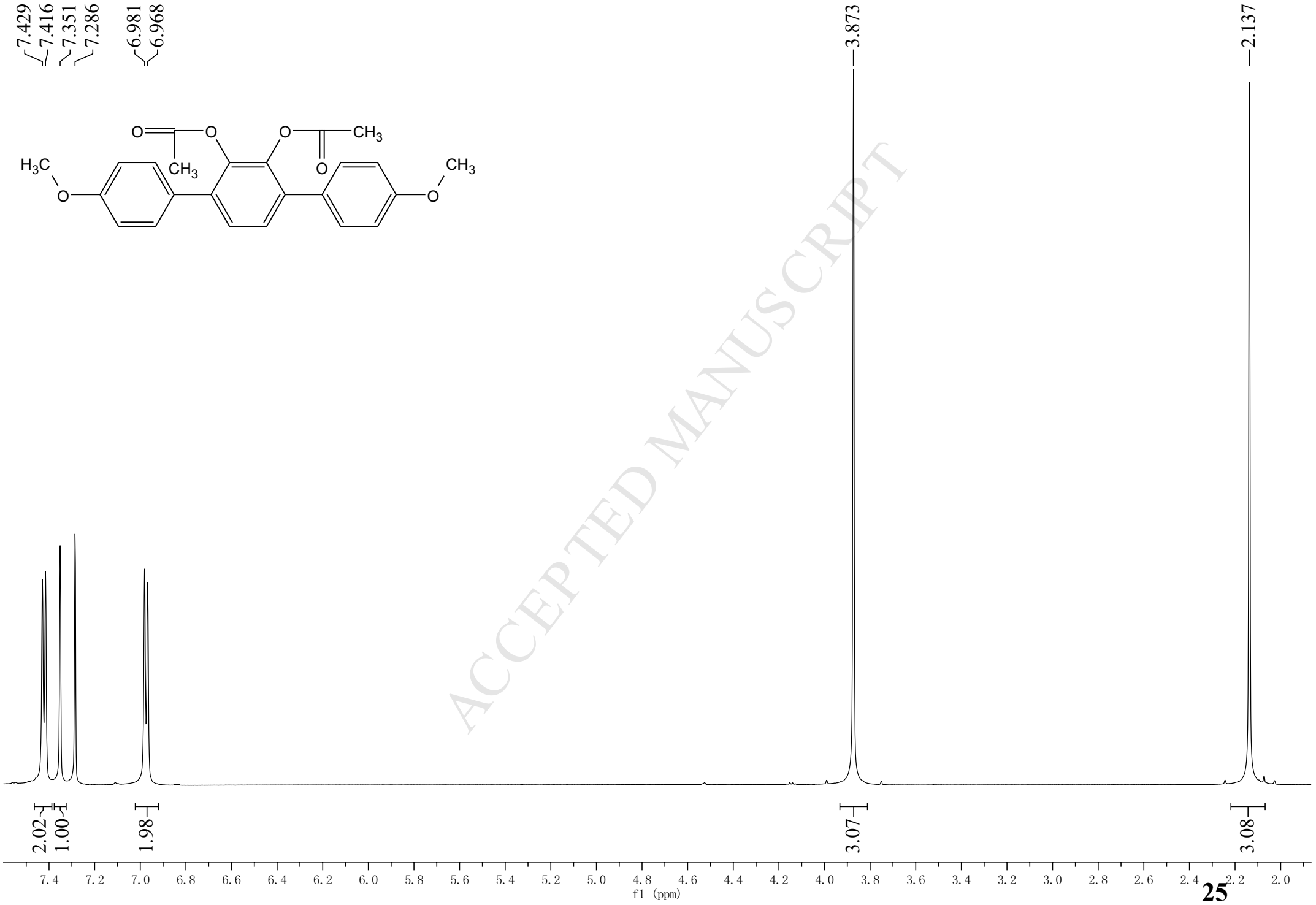

^{13}C NMR (150 MHz, $CDCl_3$, rt) of **13**

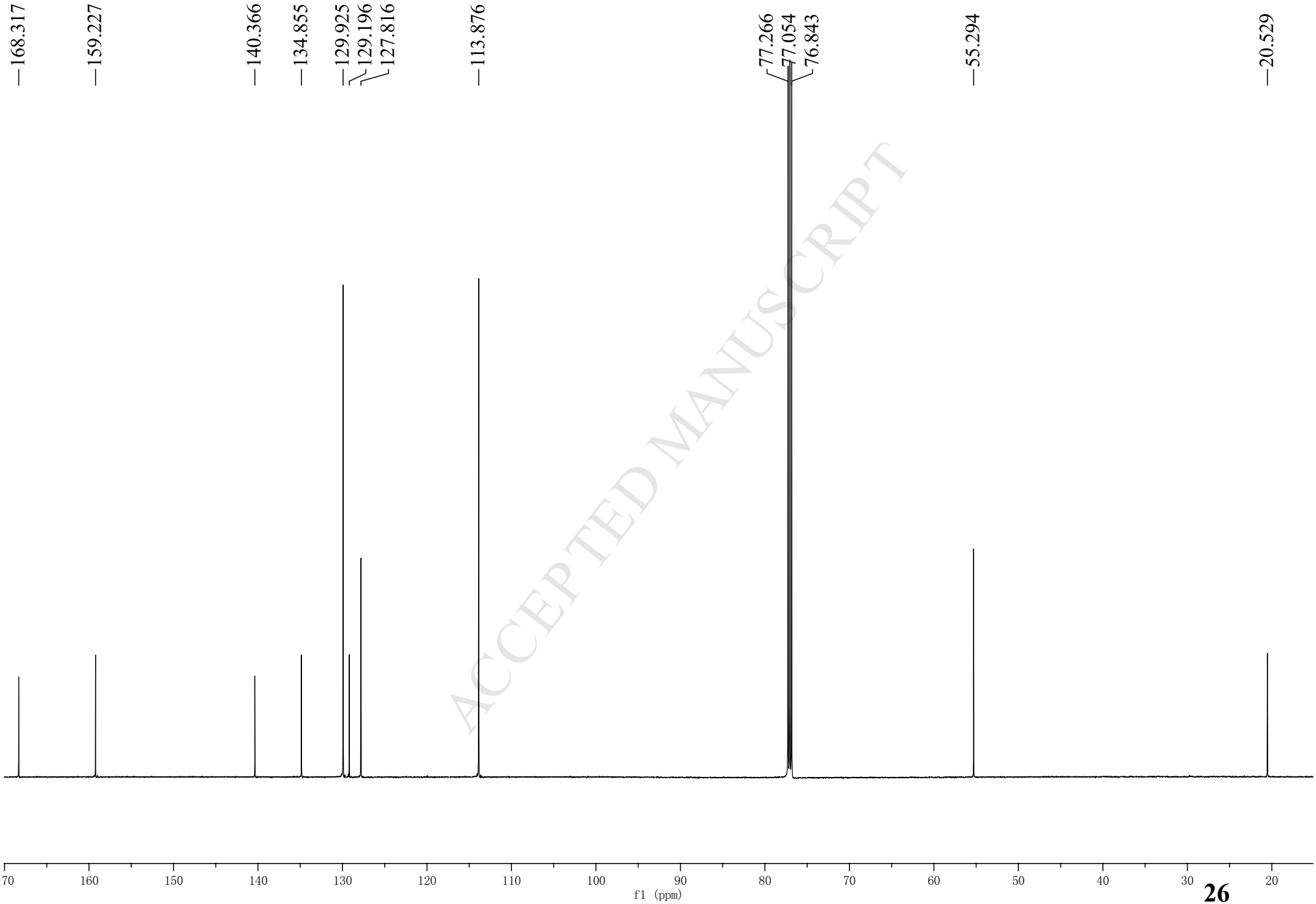

^{1}H NMR (600 MHz, $CDCl_3$, rt) of **14**

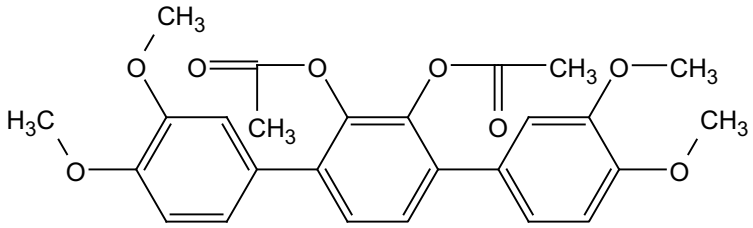

^{13}C NMR (150 MHz, $CDCl_3$, rt) of **14**

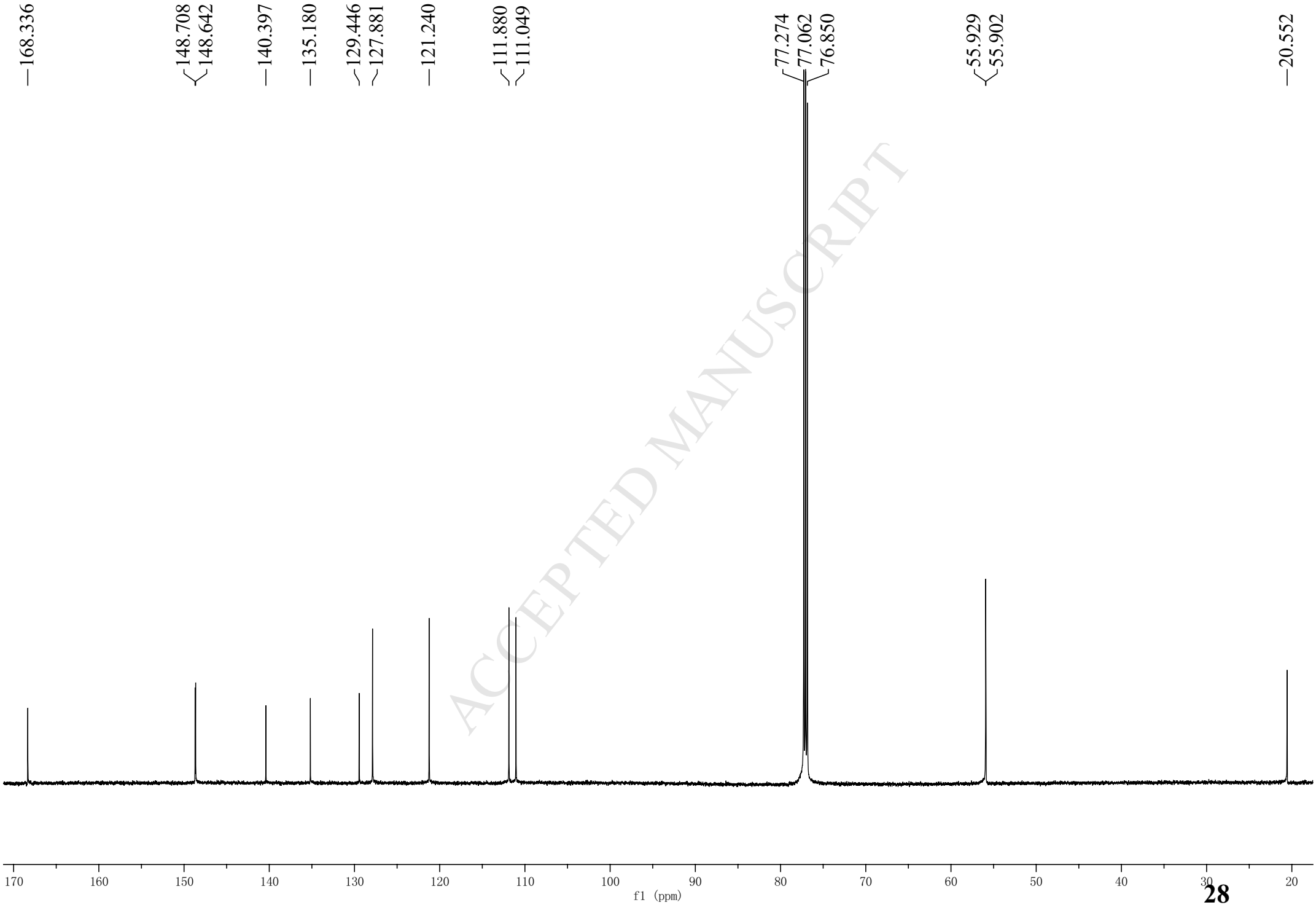

^{1}H NMR (600 MHz, $(CD_3)_2CO$, rt) of **15**

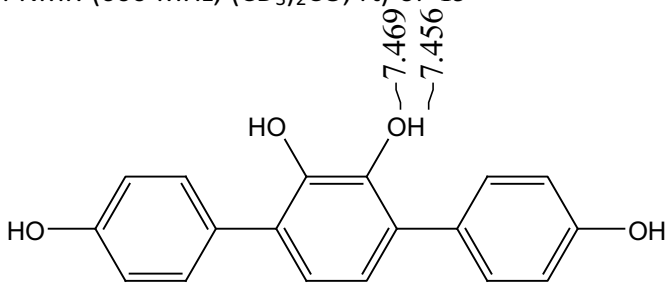

^{13}C NMR (150 MHz, $(CD_3)_2CO$, rt) of **15**

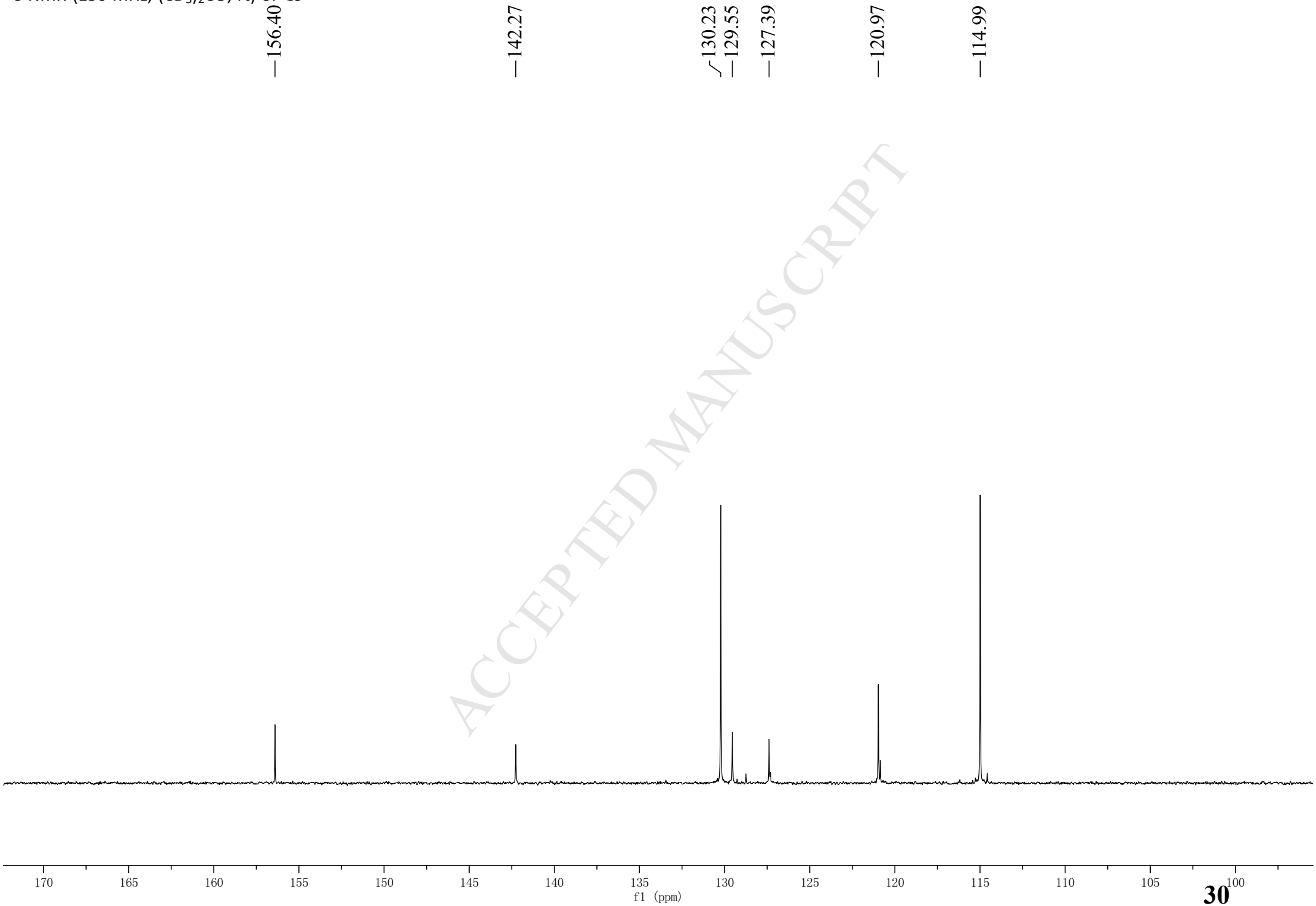

^{1}H NMR (600 MHz, $(CD_3)_2CO$, r.t.) of **16**

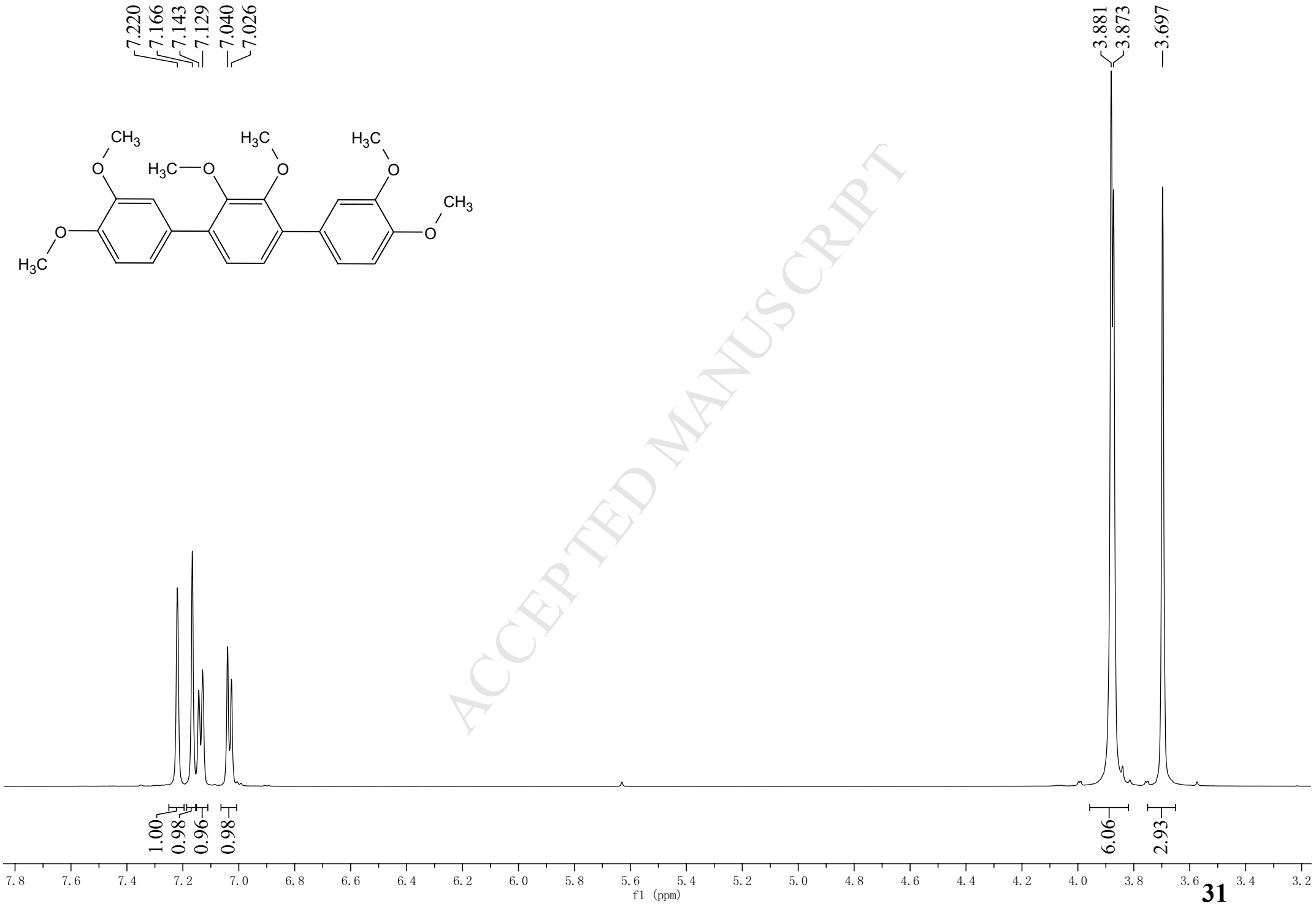

^{13}C NMR (150 MHz, $(CD_3)_2CO$, r.t.) of **16**

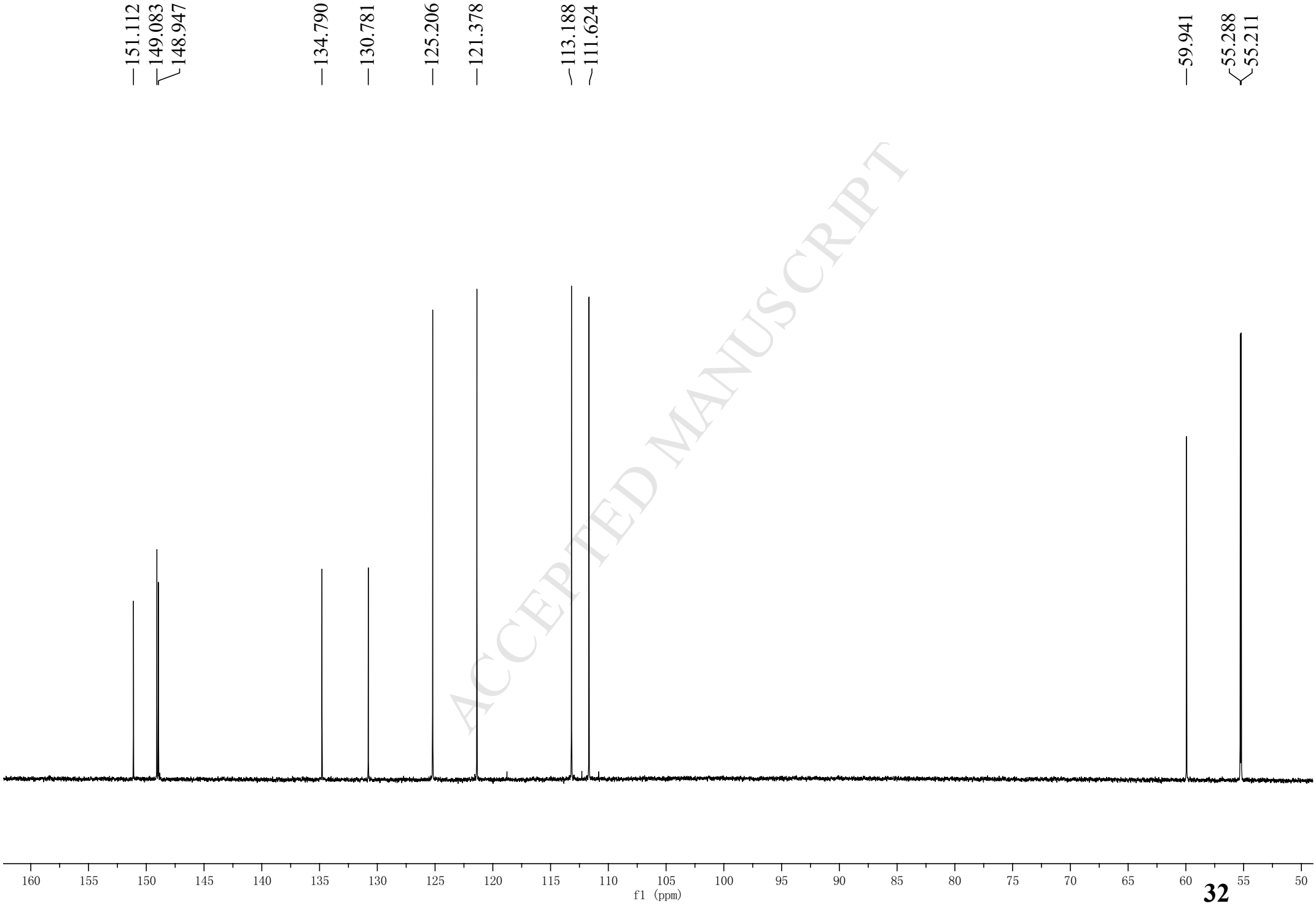

^{1}H NMR (600 MHz, $(CD_3)_2CO$, rt) of **17**

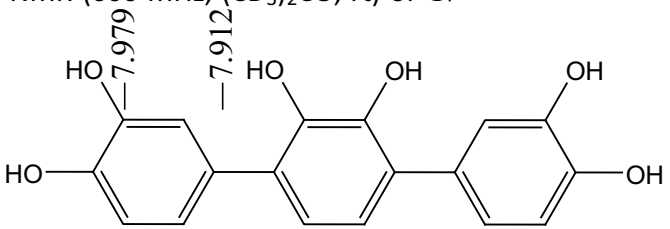

^{13}C NMR (150 MHz, $(CD_3)_2CO$, rt) of **17**

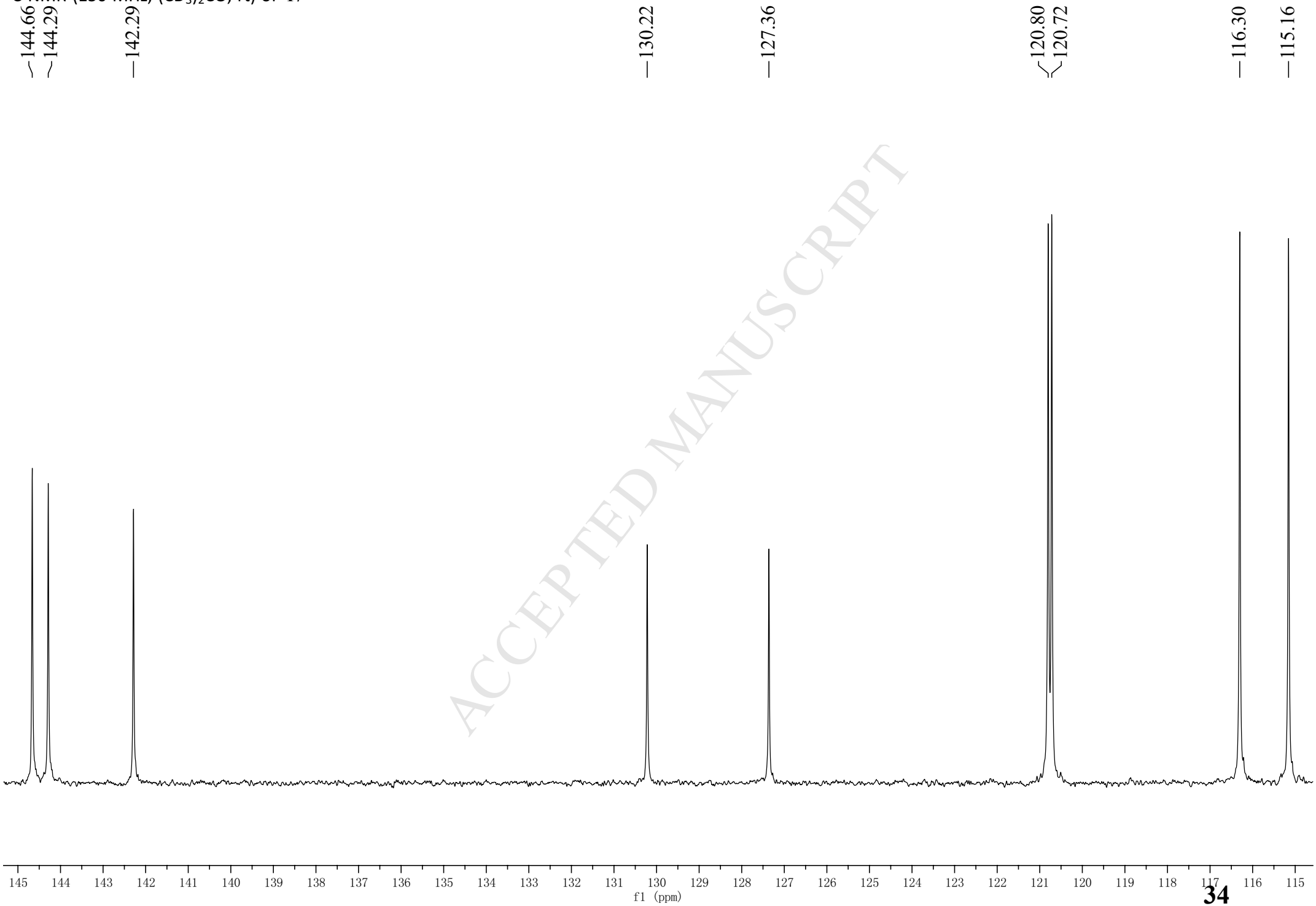

^{1}H NMR (600 MHz, $CDCl_3$, rt) of **18**

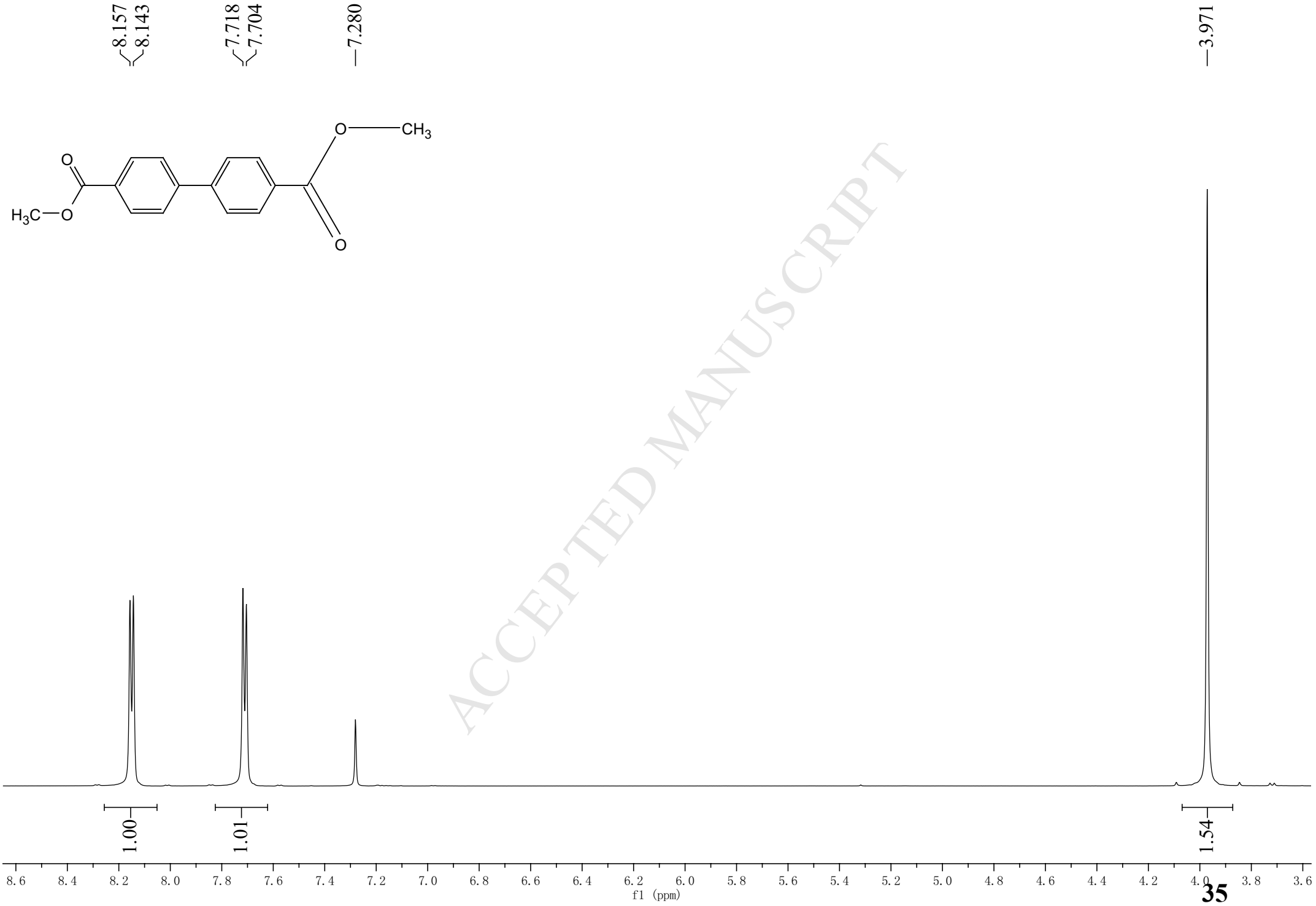

^{13}C NMR (150 MHz, $CDCl_3$, rt) of **18**

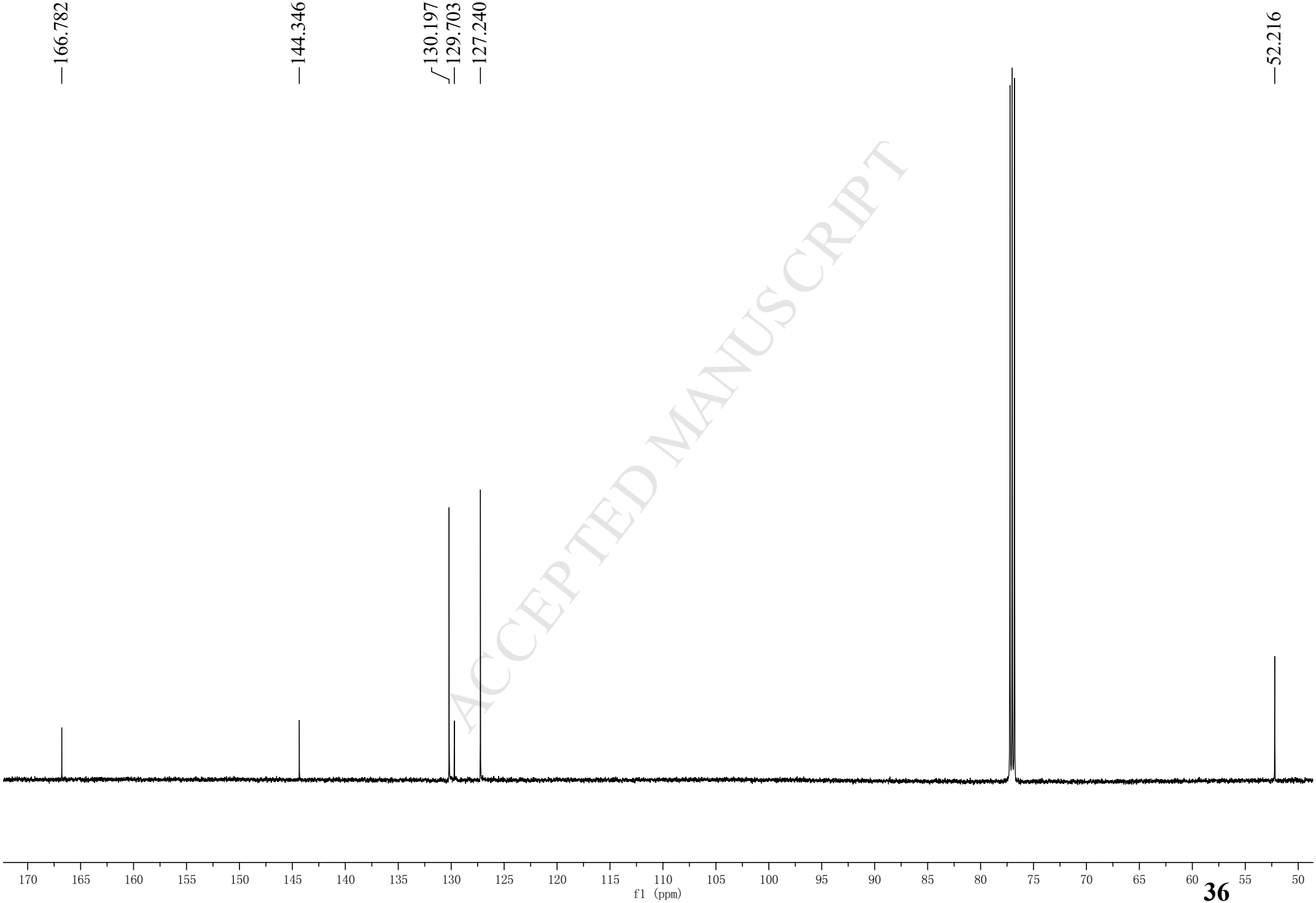

^{1}H NMR (600 MHz, $(CD_3)_2CO$, rt) of **19**

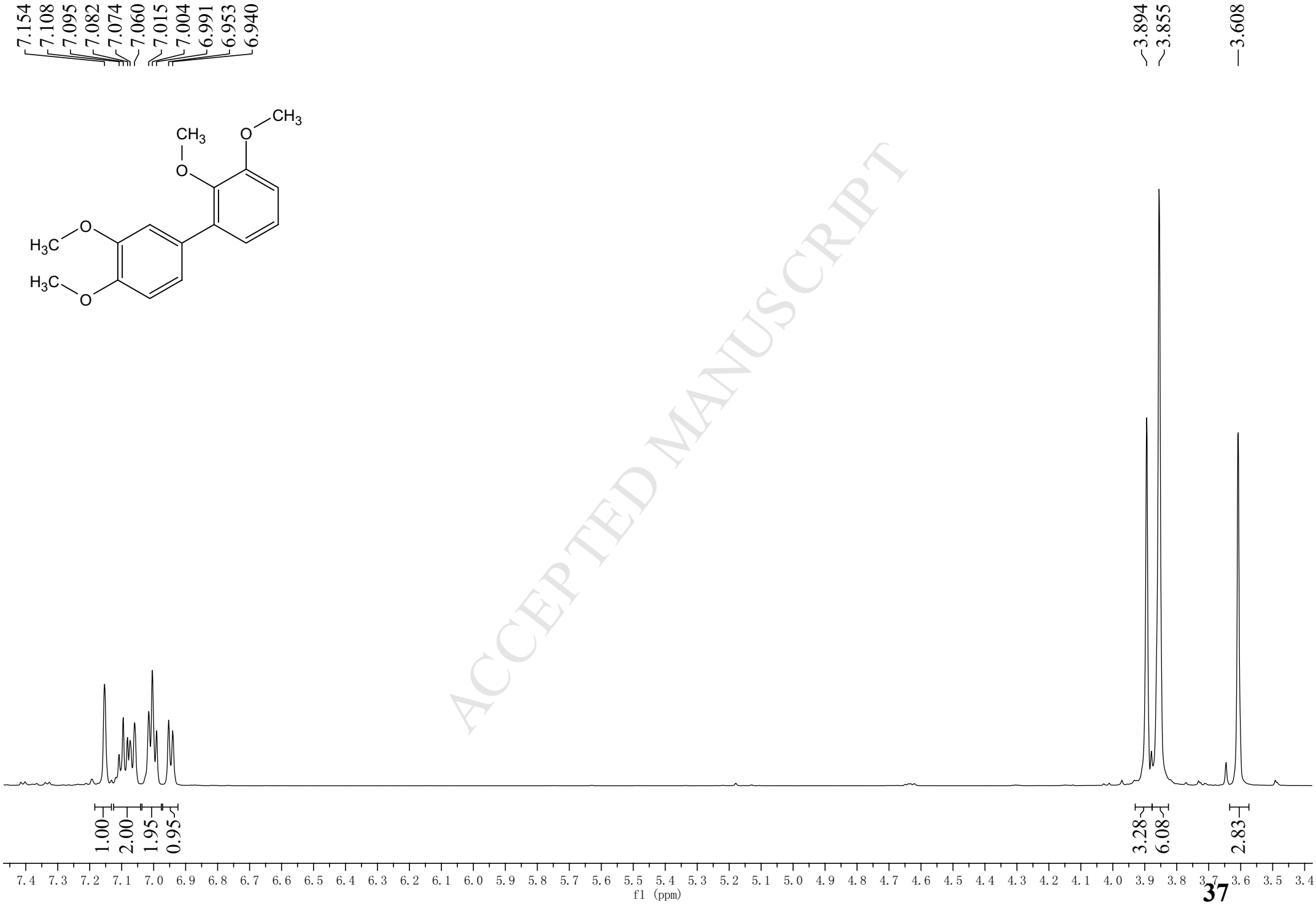

^{13}C NMR (150 MHz, $(CD_3)_2CO$, rt) of **19**

153.446
148.933
148.805
146.582
135.518
131.091
123.889
122.191
121.430
113.354
111.571
59.558
55.321
55.241
55.192

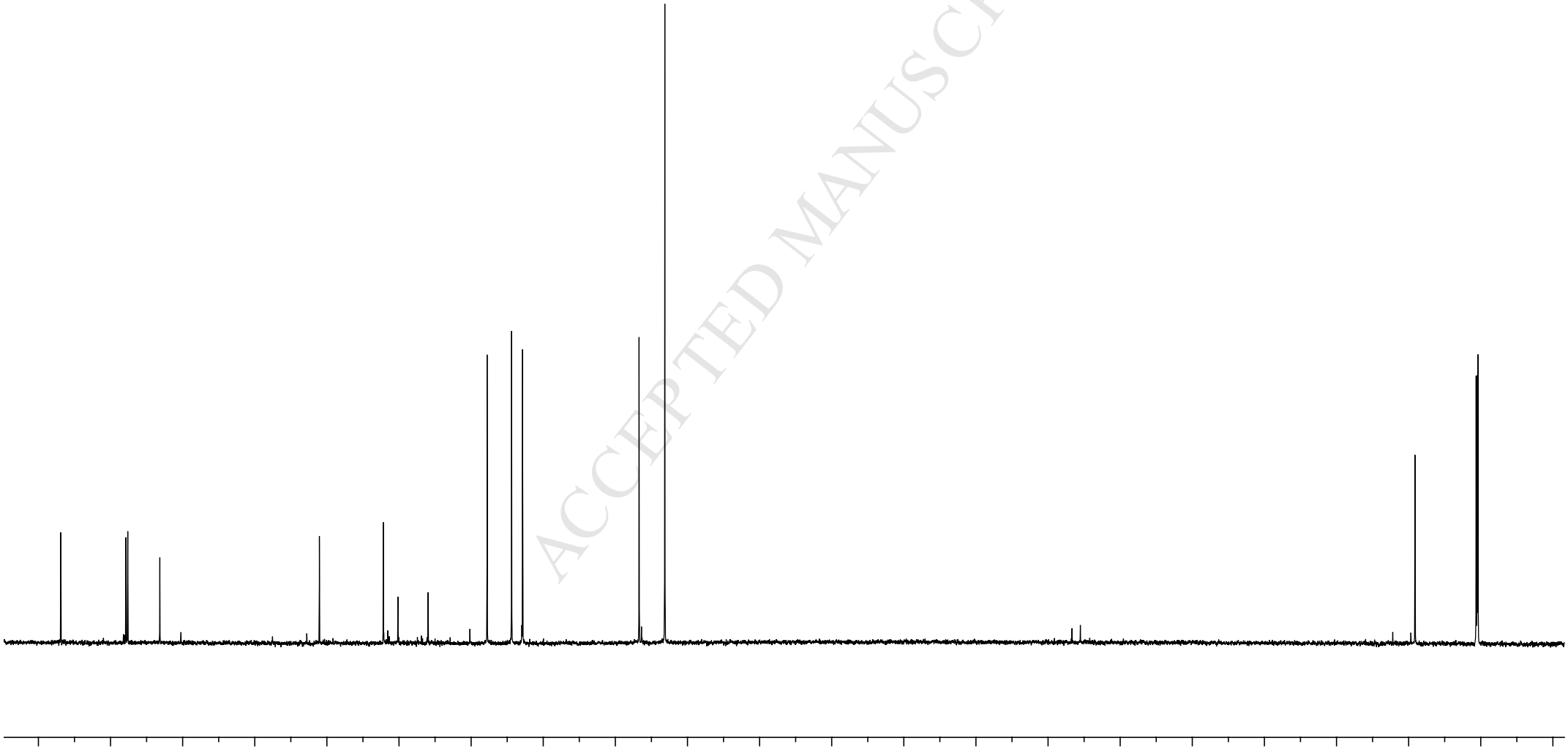

^{1}H NMR (600 MHz, DMSO-*d6*, rt) of **20**

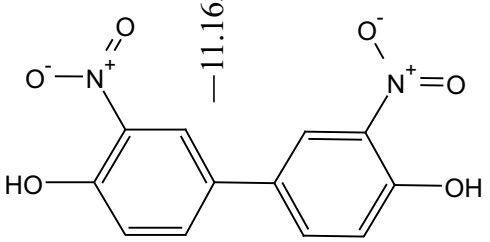

^{13}C NMR (150 MHz, DMSO-*d6*, rt) of **20**

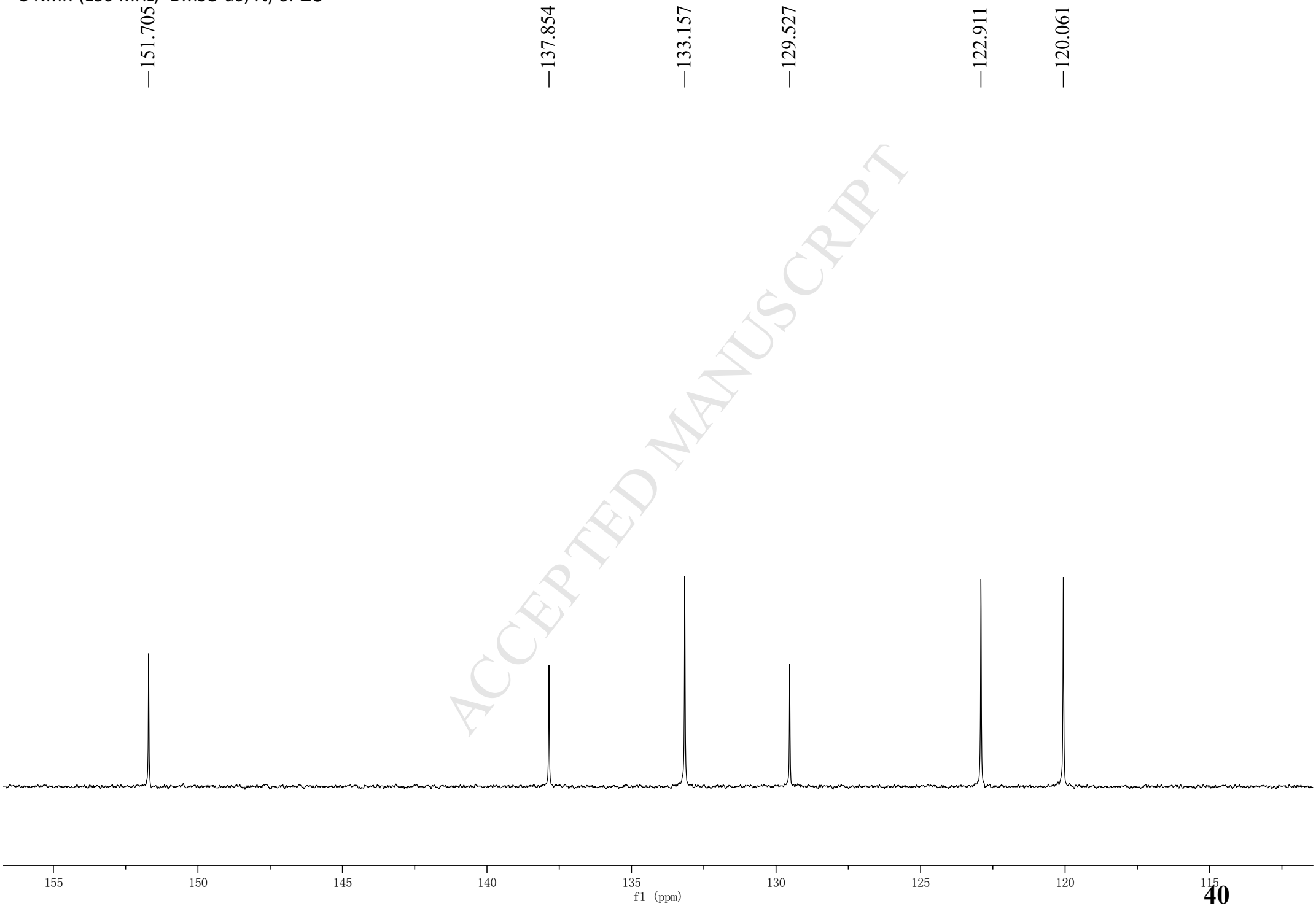

^{1}H NMR (600 MHz, $CDCl_3$, rt) of **21**

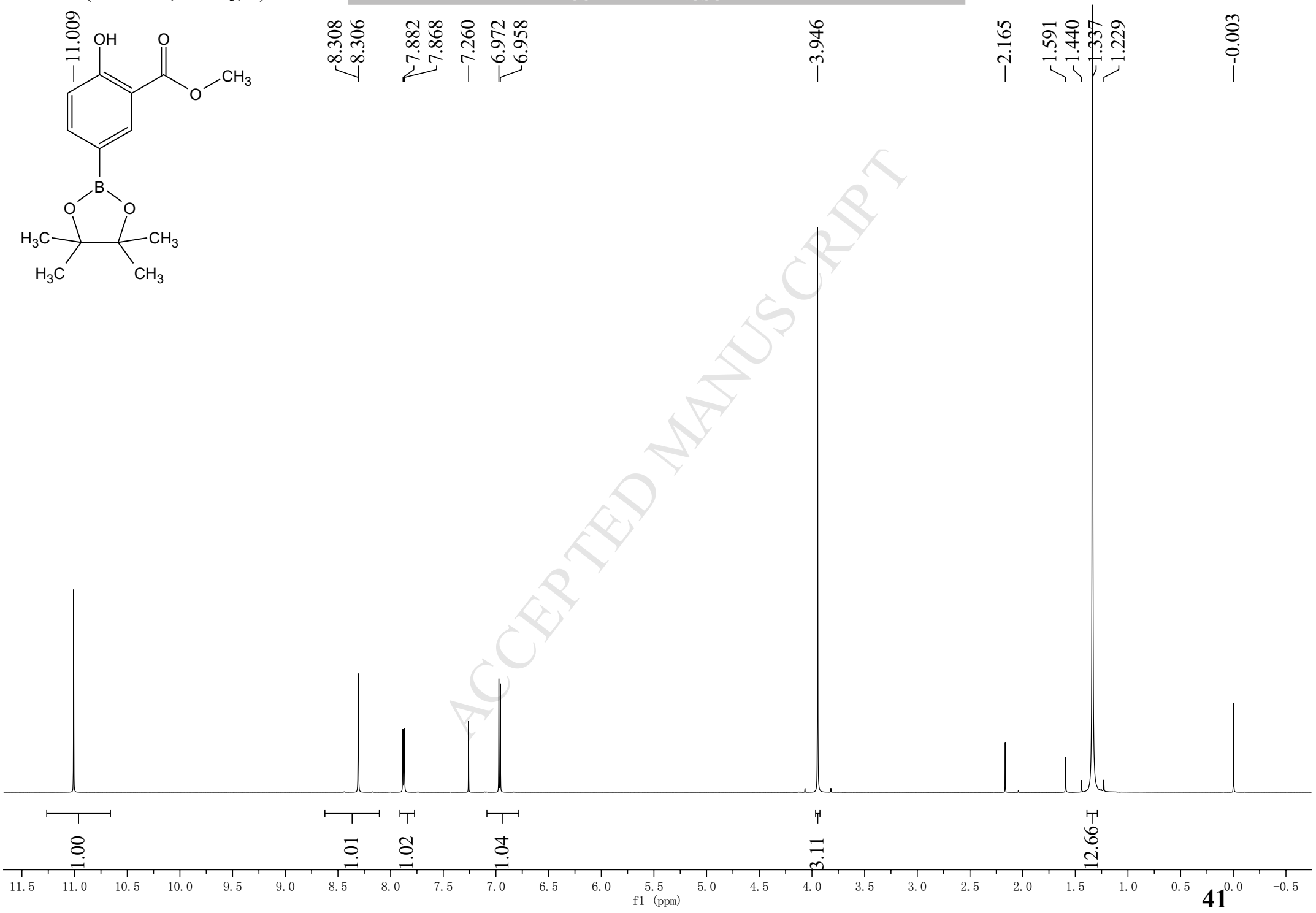

^{13}C NMR (150 MHz, $CDCl_3$, rt) of **21**

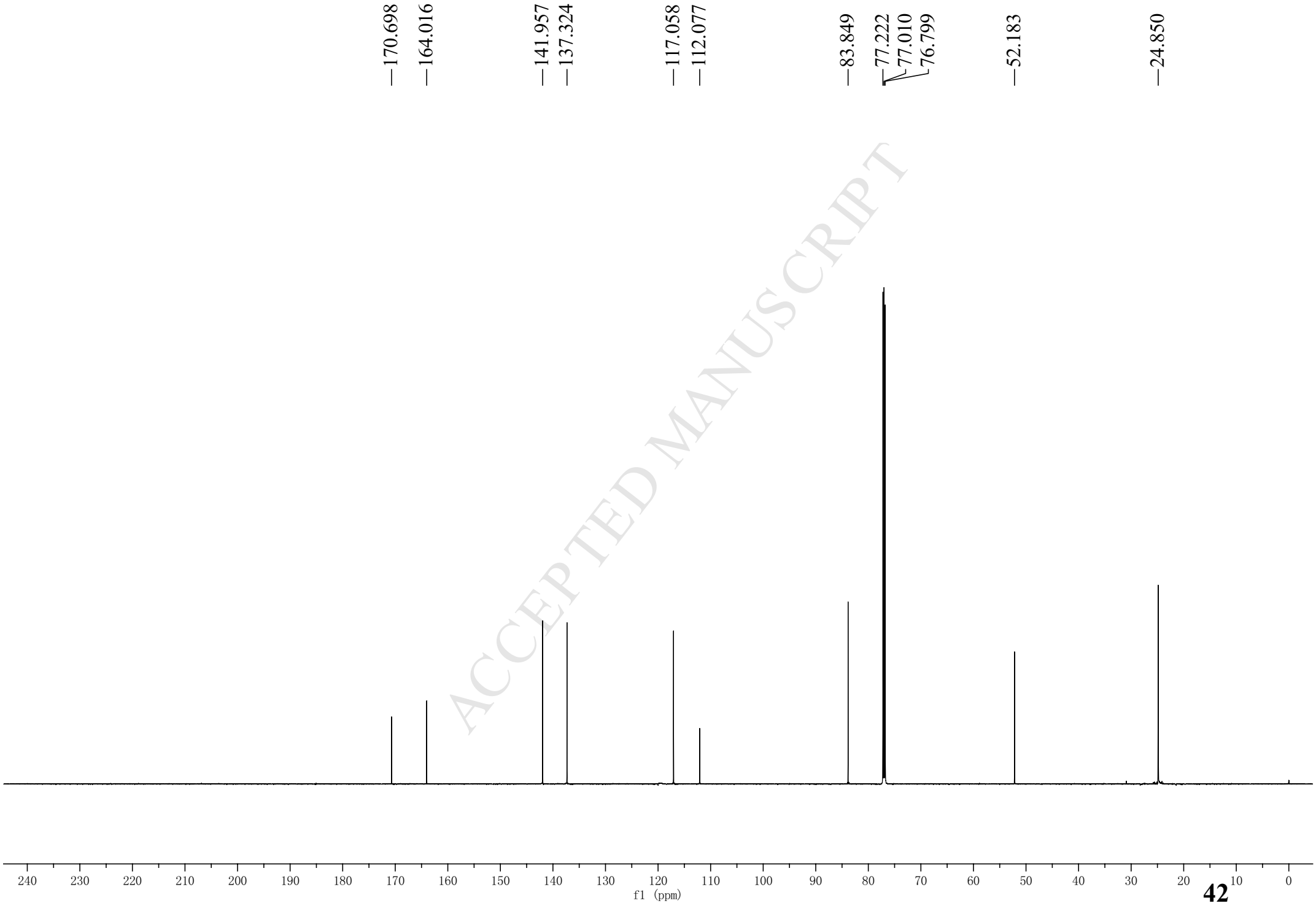

^{1}H NMR (600 MHz, $CDCl_3$, rt) of **22**

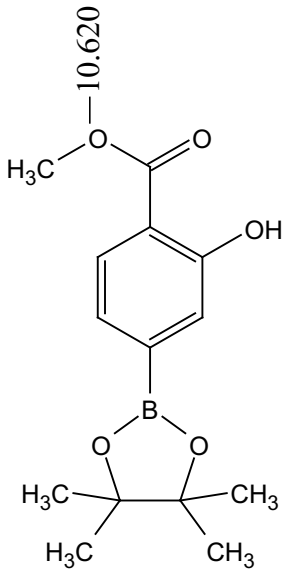

^{1}H NMR (600 MHz, $(CD_3)_2CO$, rt) of **25**

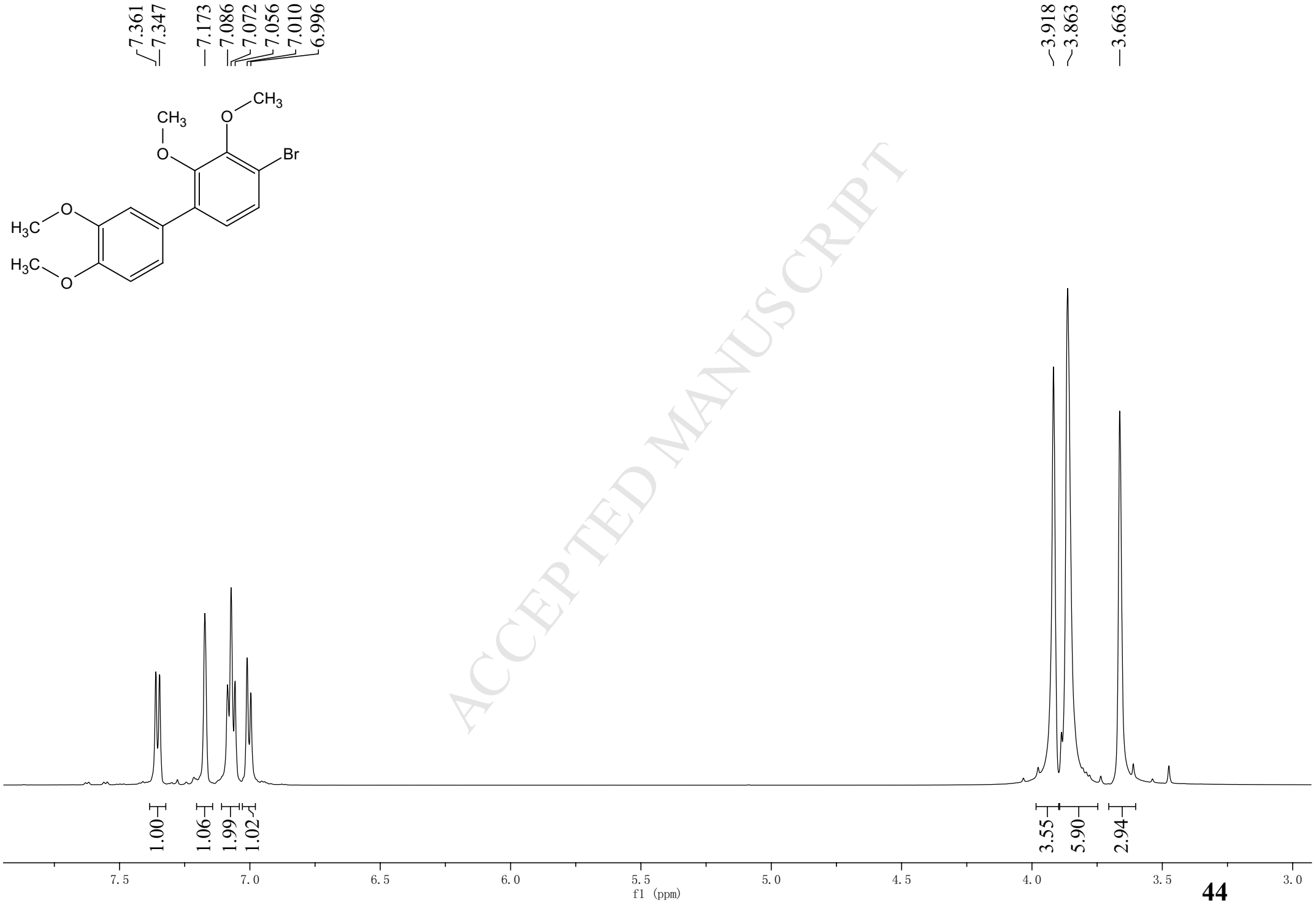

^{13}C NMR (150 MHz, $(CD_3)_2CO$, rt) of **25**

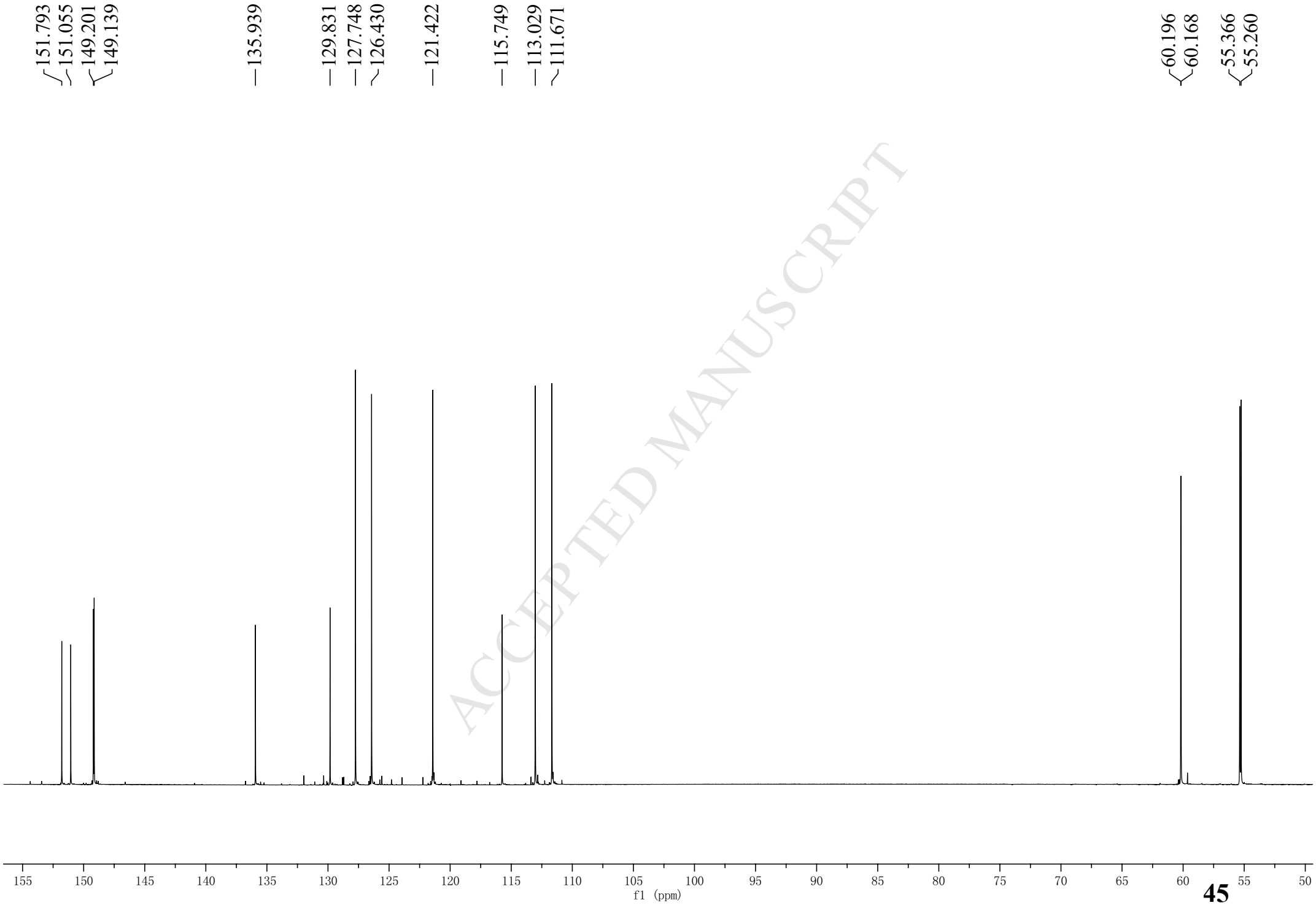

^{1}H NMR (600 MHz, $CDCl_3$, rt) of **30**

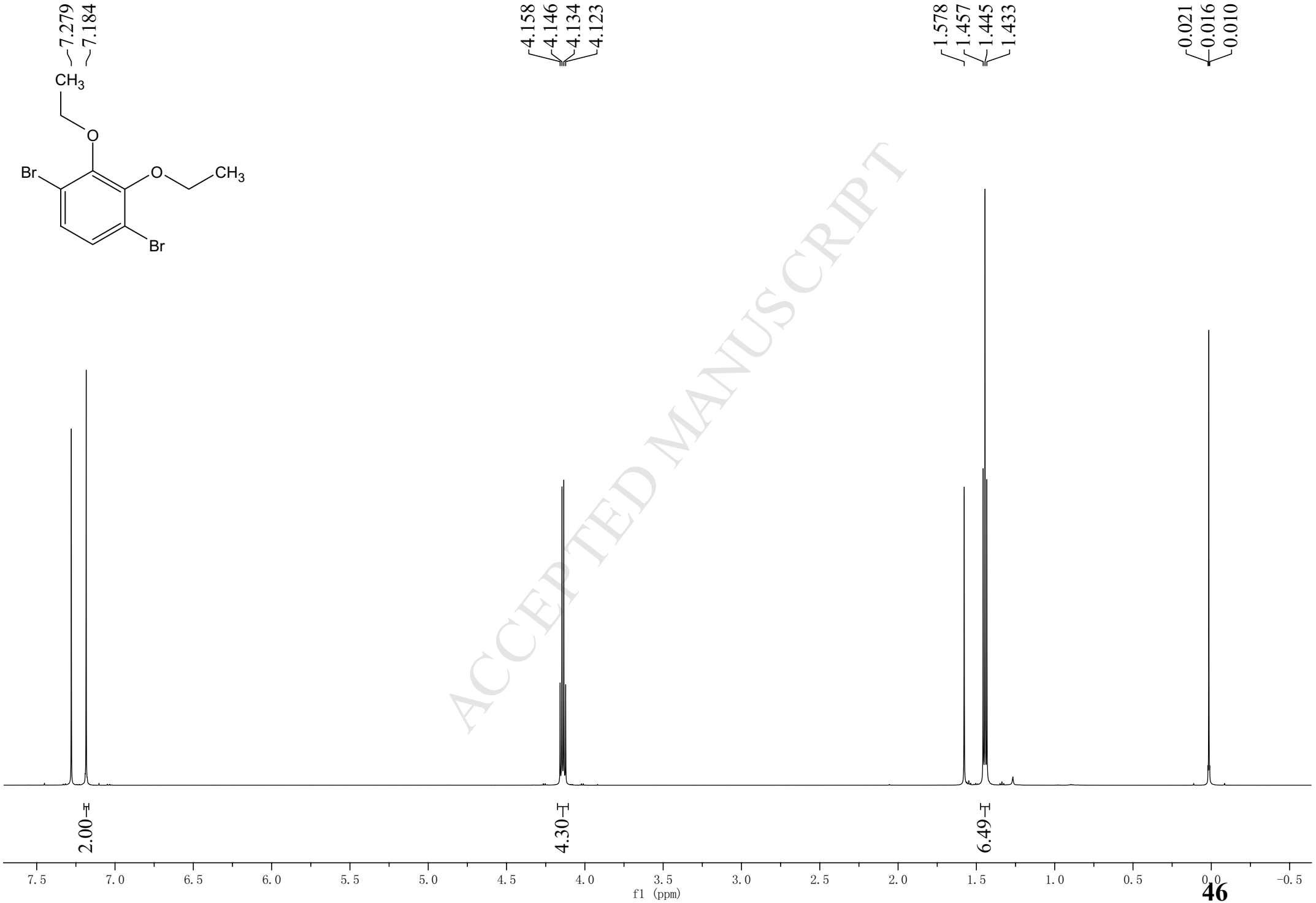

^{13}C NMR (150 MHz, $CDCl_3$, rt) of **30**